

THIS REPORT HAS BEEN DELIMITED
AND CLEARED FOR PUBLIC RELEASE
UNDER DOD DIRECTIVE 5200,20 AND
NO RESTRICTIONS ARE IMPOSED UPON
ITS USE AND DISCLOSURE.

DISTRIBUTION STATEMENT A

APPROVED FOR PUBLIC RELEASE;
DISTRIBUTION UNLIMITED.

Armed Services Technical Information Agency

Because of our limited supply, you are requested to return this copy WHEN IT HAS SERVED YOUR PURPOSE so that it may be made available to other requesters. Your cooperation will be appreciated.

AD

38641

NOTICE: WHEN GOVERNMENT OR OTHER DRAWINGS, SPECIFICATIONS OR OTHER DATA ARE USED FOR ANY PURPOSE OTHER THAN IN CONNECTION WITH A DEFINITELY RELATED GOVERNMENT PROCUREMENT OPERATION, THE U. S. GOVERNMENT THEREBY INCURS NO RESPONSIBILITY, NOR ANY OBLIGATION WHATSOEVER; AND THE FACT THAT THE GOVERNMENT MAY HAVE FORMULATED, FURNISHED, OR IN ANY WAY SUPPLIED THE SAID DRAWINGS, SPECIFICATIONS, OR OTHER DATA IS NOT TO BE REGARDED BY IMPLICATION OR OTHERWISE AS IN ANY MANNER LICENSING THE HOLDER OR ANY OTHER PERSON OR CORPORATION, OR CONVEYING ANY RIGHTS OR PERMISSION TO MANUFACTURE, USE OR SELL ANY PATENTED INVENTION THAT MAY IN ANY WAY BE RELATED THERETO.

Reproduced by
DOCUMENT SERVICE CENTER
KNOTT BUILDING, DAYTON, 2, OHIO

UNCLASSIFIED

A Reprint from

SELECTED

COMBUSTION PROBLEMS

Fundamental and Aeronautical Applications

ADVISORY GROUP FOR
AERONAUTICAL RESEARCH AND DEVELOPMENT
NORTH ATLANTIC TREATY ORGANIZATION
PALAIS DE CONGRÈS
PARIS

Published by
BUTTERWORTES SCIENTIFIC PUBLICATIONS
88 KINGSWAY, LONDON, W.C.2

EXPERIMENTAL STUDIES ON TURBULENT FLAMES*

ARCH C. SCURLOCK and JOHN H. GROVER

Atlantic Research Corporation

Both turbulent diffusion flames and turbulent flames propagating in homogeneous mixtures are considered. For turbulent diffusion flames, typical experimental results are reviewed which establish that mixing, principally by eddy diffusion, controls the burning process. For both confined and unconfined turbulent flames propagating in homogeneous mixtures, the limited experimental results useful for comparison with theory are reviewed. Demonstrated are: the magnitude of the increase in flame velocity resulting from turbulence, the increase in flame distortion and in turbulent flame velocity with distance downstream from the stabilizer, the characteristic structure of the instantaneous flame front, and, for confined flames, the presence of flame-generated turbulence. The experimental results are compared with a theory for the effect of large-scale turbulence, previously developed by the authors, which assumes that turbulence only wrinkles the flame front without changing S_L , and relates S_T/S_L to the dimensionless parameters v'/S_L , ρ_u/ρ_b , and $S_L l/l_2$. Three effects are taken into account in the theory: eddy diffusion, flame propagation, and flame-generated turbulence. Agreement of theory and experiment is acceptable in some instances, but in others the need for further refinement of the theory is evident. Indicated refinements include provision for effects of flame curvature and of flame front instability (when it exists) on S_T , provision for effect of 'flame Reynolds number' on percentage conversion of available energy to turbulence, and provision for the effect on S_T of nonisotropy of the flame-generated turbulence. Additional experimental work is necessary to establish the exact nature of these effects. Experimental approaches which should yield useful data are suggested. Consideration of the effect of rate of increase of turbulent flame area in decreasing S_L indicates only a very small reduction even under extreme conditions. The possibility is discussed that at very high, but obtainable, volumetric heat release rates the combustion process may approach that of homogeneous chemical reaction and that under these conditions chemical reaction rate may become controlling.

THAT turbulence increases the rate of burning in combustible mixtures has long been known, receiving qualitative recognition by MALLARD and LE CHATELIER¹⁶ as early as 1883 on the basis of their flame studies, and the enormous volumetric burning rates often attained in jet and internal combustion engines are attributed to the presence of turbulence.

Turbulent flames may be divided into two broad categories—turbulent diffusion flames and turbulent flames propagating in homogeneous mixtures. Although in practice mixed flames which are some sort of combination of these two flame types are frequently encountered, the effects of turbulence on the two types appear to be quite different.

* This paper was prepared under the auspices of Project SQUID, jointly sponsored by the Office of Naval Research and the Office of Air Research under Contract NONr-485(01).

TURBULENT COMBUSTION

TURBULENT DIFFUSION FLAMES

In a diffusion flame the fuel and oxidant gases are initially separated. Thus for combustion to take place, mixing of the two components is first necessary. For laminar diffusion flames, the importance of molecular diffusion in effecting this mixing process has been demonstrated by BURKE and SCHUMANN⁴ and by HOTTEL and HAWTHORNE¹⁰.

It may also be concluded from the literature that the mixing of fuel and oxidant by eddy diffusion is the principal controlling factor determining the rate of burning of turbulent diffusion flames. The work reported by HAWTHORNE, WEDDELL and HOTTEL⁸, by WOHL, GAZLEY and KAPP³², and by HOTTEL⁹ with turbulent fuel jets issuing into stagnant air and with liquid jets of alkali discharging into a reservoir of acid has greatly enhanced our knowledge of turbulent diffusion flames, and several important conclusions may be reached from these investigations. Fig. 1, after Hottel and Hawthorne¹⁰, is a schematic diagram showing the progressive change in the

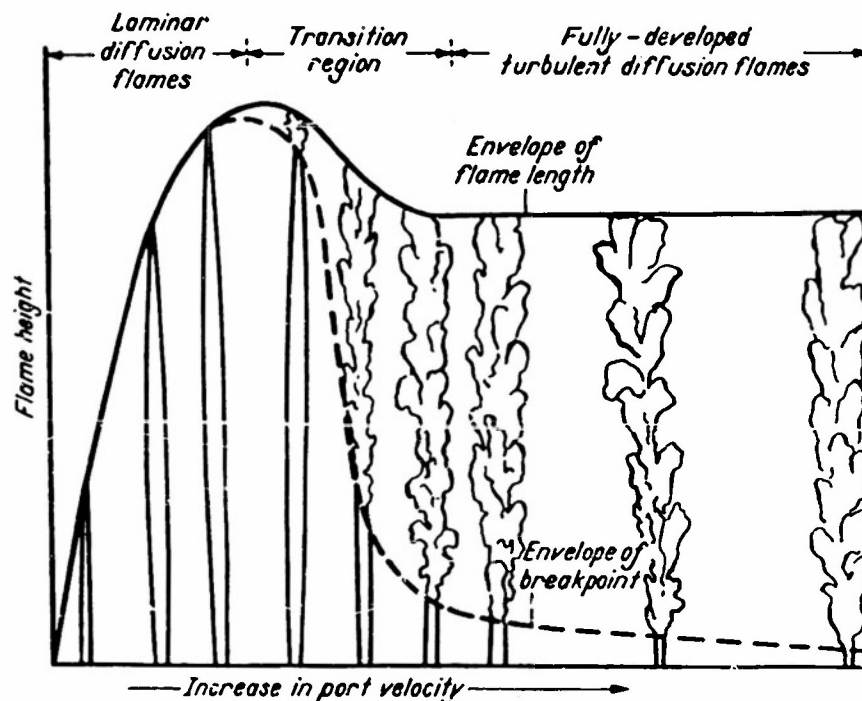


Fig. 1. Progressive change in flame with increase in port velocity (from HOTTEL and HAWTHORNE¹⁰)

diffusion flame with increase in burner port velocity. As port velocity of the laminar diffusion flame is increased, the flame length also increases until eddies begin to appear at the flame tip. Further increase in velocity causes the point of initiation of the eddies to move down along the flame, causing the overall flame length to shorten and dividing the flame into a laminar section near the burner port and a turbulent brush. Fig. 2, after Hottel⁹ based on the data of GAUNCE⁷ for city-gas flames, shows the effect of burner port velocity on flame height to near sonic velocity. Fig. 3 from Wohl, Gazley and Kapp³² shows the relationship between flame height, port diameter, and port velocity for 50 per cent city gas issuing into stagnant air. The insensitivity of the height of fully-developed turbulent diffusion flame jets to burner port velocity is clearly illustrated.

EXPERIMENTAL STUDIES ON TURBULENT FLAMES

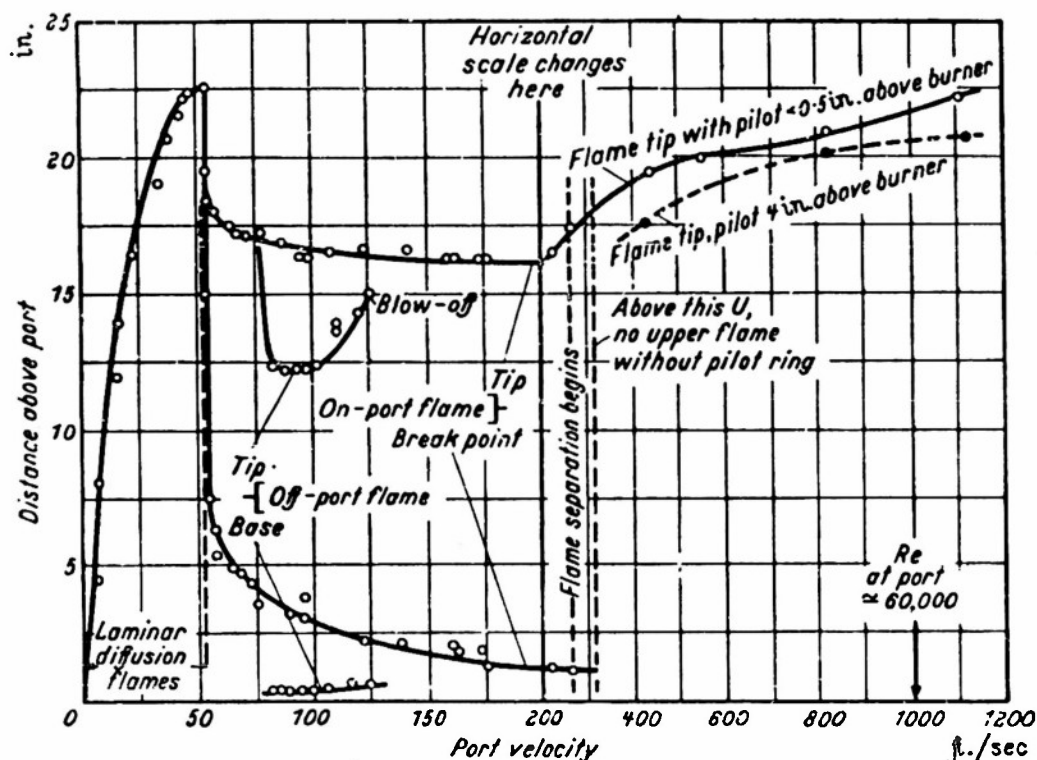


Fig. 2. Effect of port velocity on flame height (from HOTTEL⁹ based on data of GAUNCE⁷ for city gas flames: burner port diameter $\frac{1}{8}$ in.)

Observation of the remarkable similarity of the jet structure of turbulent diffusion flames, of similar jets in the absence of combustion, and of alkali jets discharging into a reservoir of acid led Hawthorne, Weddell and Hottel⁸, and Hottel⁹ to conclude that for fully-developed turbulent diffusion

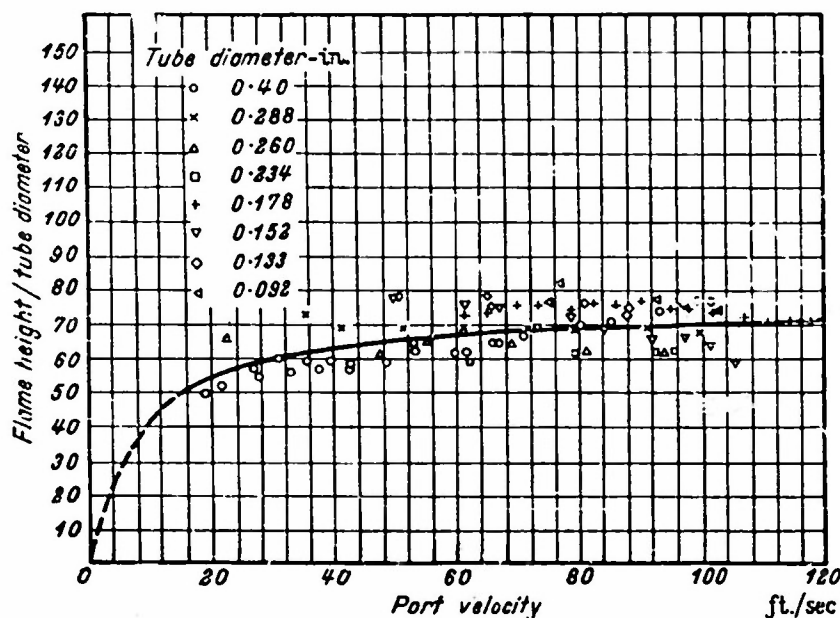


Fig. 3. Correlation of flame height of fully-developed turbulent diffusion flames with port diameter and port velocity for jets of 50 per cent city gas issuing into stagnant air, after WOHL, GAZLEY, and KAP¹²

TURBULENT COMBUSTION

flame jets the process of mixing, which is a function of the momentum and buoyancy of the jet, is the controlling factor in determining the progress of the combustion. There is no evidence with these flames that the combustion process itself results in additional turbulence generation.

If mixing by eddy diffusion is the controlling factor determining the height H of the fully-developed turbulent jet, then H should be inversely proportional to the eddy diffusivity ϵ , directly proportional to volumetric flow rate from the jet which is in turn proportional to the product of port diameter D squared and port velocity U , inversely proportional to the fuel-oxidant interface area per unit of jet length which is proportional to D , and inversely proportional to the concentration gradient normal to the area across which eddy diffusion proceeds which is inversely proportional to D .

In accordance with the theory of turbulent mixing, it may be assumed that eddy diffusivity is proportional to the product of turbulence intensity v' and scale l_2 . In a turbulent jet the assumption that l_2 at any point is proportional

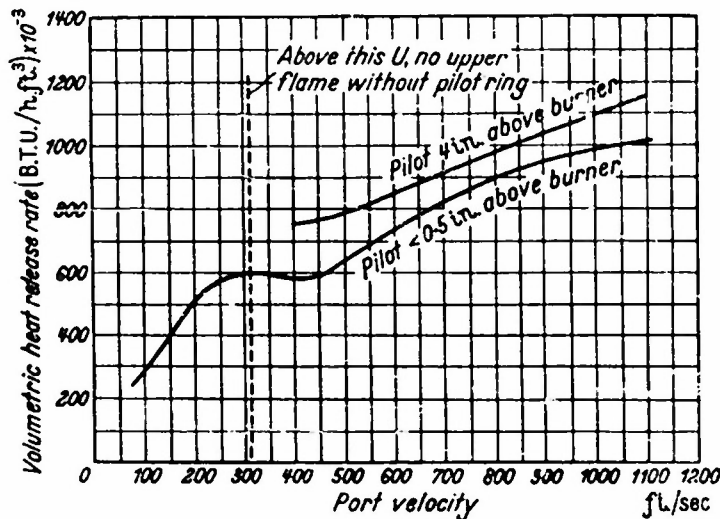


Fig. 4. Volumetric heat release rate as a function of port velocity for the turbulent diffusion flame jet of Fig. 2: lower heating value of fuel taken as 8,830 B.T.U./lb.

to the port diameter D , and that v' is proportional to the jet velocity U is known to be a good approximation⁸. Thus the following may be written:

$$H \propto \frac{1}{\epsilon} \cdot UD^2 \cdot \frac{1}{D} \cdot \frac{1}{1/D} = \frac{UD^2}{\epsilon} \propto \frac{UD^2}{UD} = D \quad \dots (1)$$

A turbulent jet height invariant with port velocity and which increases directly with port diameter is predicted. This essentially conforms with experiment.

Volumetric heat release rates for the turbulent jet of Fig. 2 have been calculated and are shown in Fig. 4*. At port velocities below about 250 ft/sec heat release rates may be said to be proportional to port velocity, which indicates that under these conditions mixing by eddy diffusion controls the rate of burning. At higher velocities the heat release rate continues to increase, but at a lower rate. This may be attributable to the assertion at these higher velocities of the influence of mixing by molecular diffusion,

* For these calculations the volume occupied by the flame was assumed to be that of a cylinder with height equal to the turbulent flame height and diameter equal to the maximum flame width. The linear relation between turbulent flame height and flame width given by Hottel⁹ was assumed.

always necessary in achieving the intimate molecular mixing of fuel and oxidant required for combustion. The heat release rate at the maximum port velocity of 1100 ft/sec reaches approximately 1.15 million B.T.U. per hour per cubic foot—a relatively low value in comparison with those often obtained with turbulent confined flames in homogeneous mixtures. Even at the highest heat release rates there is no evidence with these flames that factors other than mixing control the burning rate.*

TURBULENT FLAMES IN HOMOGENEOUS MIXTURES

As compared with turbulent diffusion flames, where mixing by eddy diffusion is the controlling factor, the mechanism of propagation of turbulent flames in homogeneous mixtures is more complex and is at the present time less well understood. The physical picture of the mechanism of propagation of such flames held by workers in the field has, in fact, until recently been so rudi-

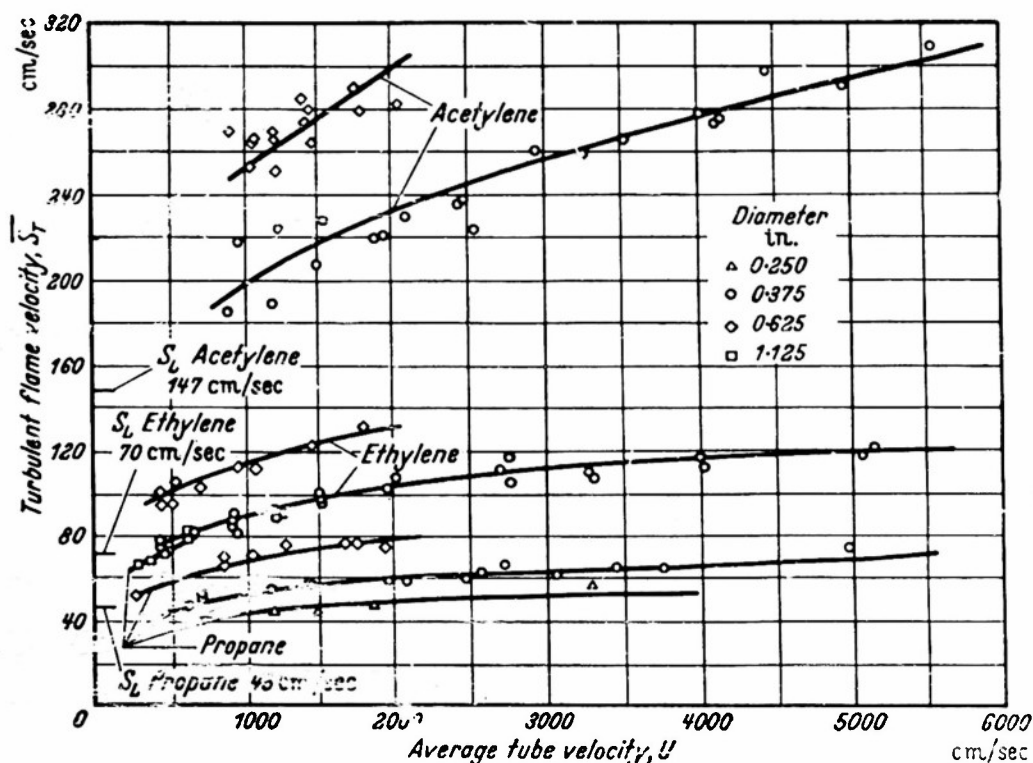


Fig. 5. Results of BOLLINGER and WILLIAMS³ for open bunsen flames disturbed by pipe turbulence, replotted as S_T versus U

mentary and the influence of the various important parameters so poorly known that theoretical considerations have been of only small assistance in planning controlled experiments. As a result of this and of the considerable difficulty involved in obtaining good data under controlled conditions with turbulent flames, the existing experimental results considered suitable for quantitative comparison with theory are extremely limited and inadequate. The principal results, those of BOLLINGER and WILLIAMS³, KARLOVITZ, DENNISTON and WELLS¹⁴, WOHL and co-workers^{29,33}, and of SCURLOCK^{21, 22} are presented in Figs. 5-9. From these figures, an idea of the importance of turbulence in increasing the rate of flame propagation may be obtained.

* And, indeed, it should not be surprising in view of the work of AVERY and HART⁸ and of LONGWELL¹⁸ (see later discussion) that chemical reaction rate exerts no controlling influence at these moderate heat release rates.

TURBULENT COMBUSTION

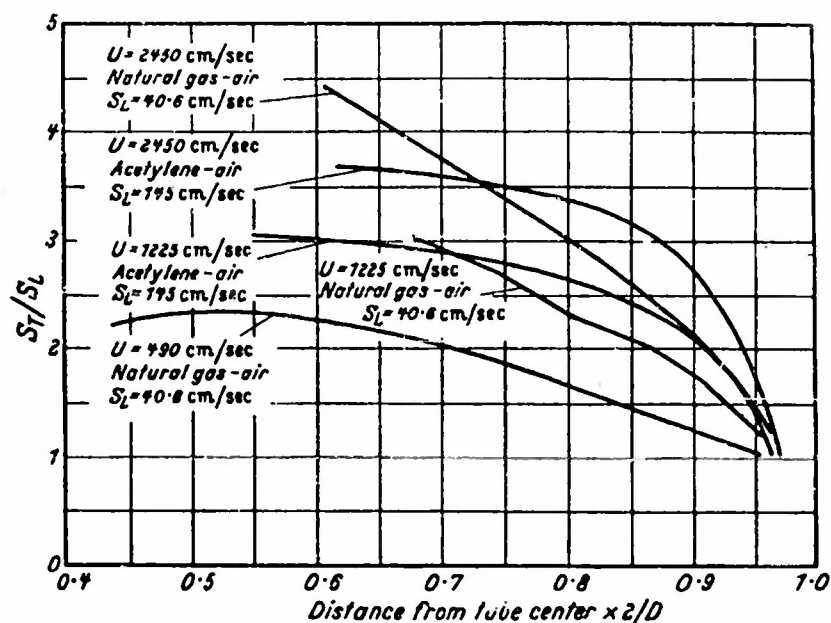


Fig. 6. Results of KARLOVITZ, DENNISTON, and WELLS¹⁴ for open bunsen flames disturbed by pipe turbulence plotted as S_T/S_L versus distance from tube center

Experimental Results

Fig. 5 presents the data of Bollinger and Williams² obtained with bunsen flames disturbed by fully-developed pipe turbulence. Acetylene, ethylene, and propane were employed in mixtures with air yielding maximum laminar flame velocity, and tube diameter was varied from 0.25 to 1.125 inches. The data have been replotted as \bar{S}_T versus U , where \bar{S}_T is the propagation velocity of the turbulent flame averaged over its entire surface. Values of laminar flame velocity S_L that were believed by Bollinger and Williams to be approximately those of the mixtures employed are also indicated. These

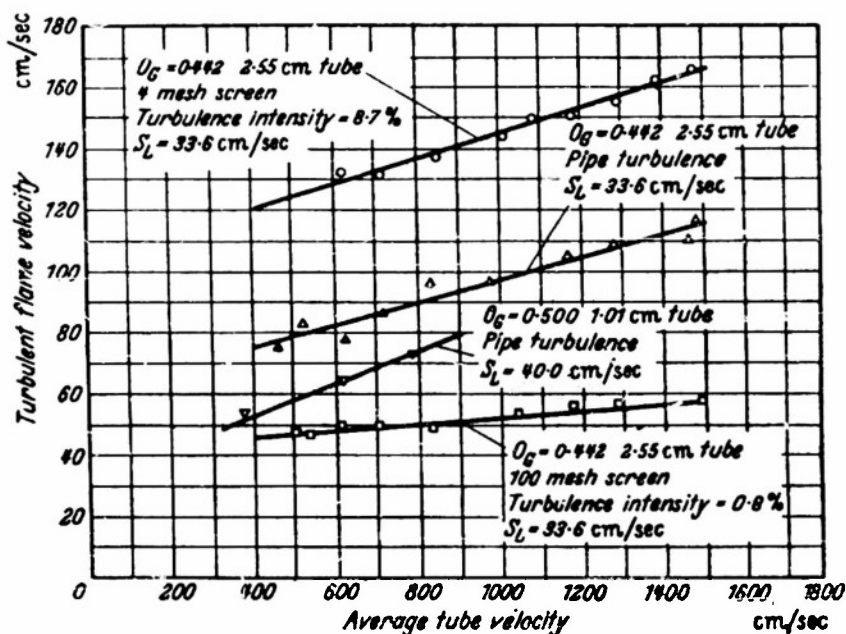


Fig. 7. Effect of tube velocity on turbulent flame velocity, after WOHL^{29,33}

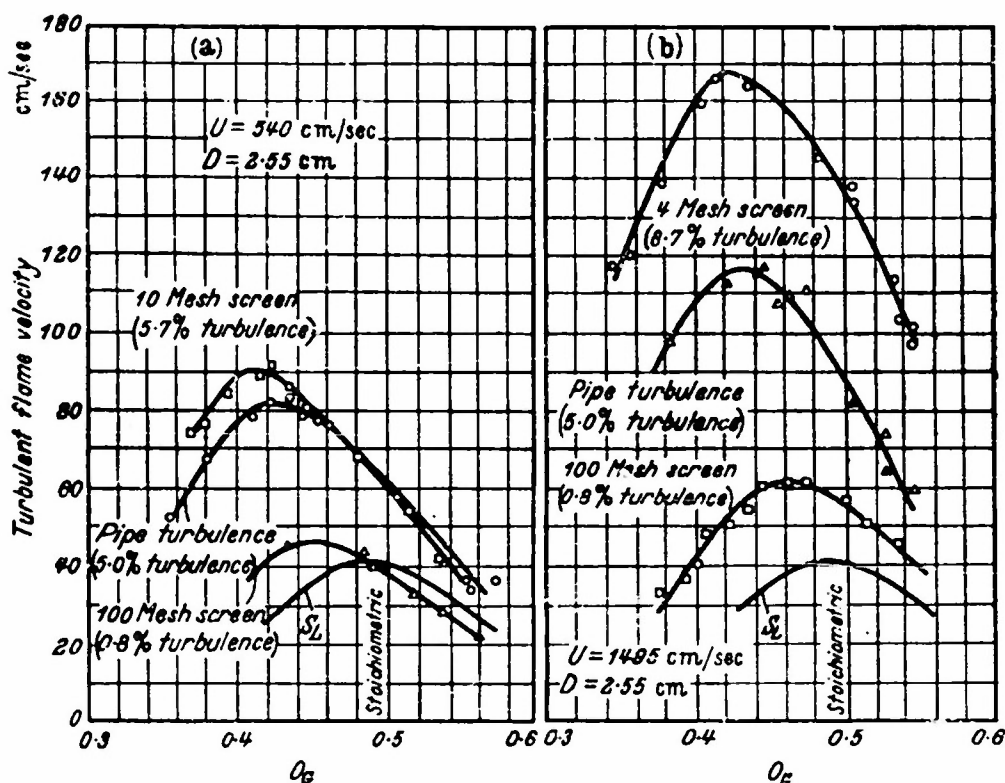


Fig. 8. Effect of mixture ratio on turbulent flame velocity for butane-air bunsen flames under various conditions of turbulence, after WOHL²²

investigators were the first to recognize that turbulent flame velocities based on the inner or outer boundary of the flame brush are more or less arbitrary*, and their determinations were thus based on the mean position of the flame, taken to be midway between the inner and outer flame boundary a

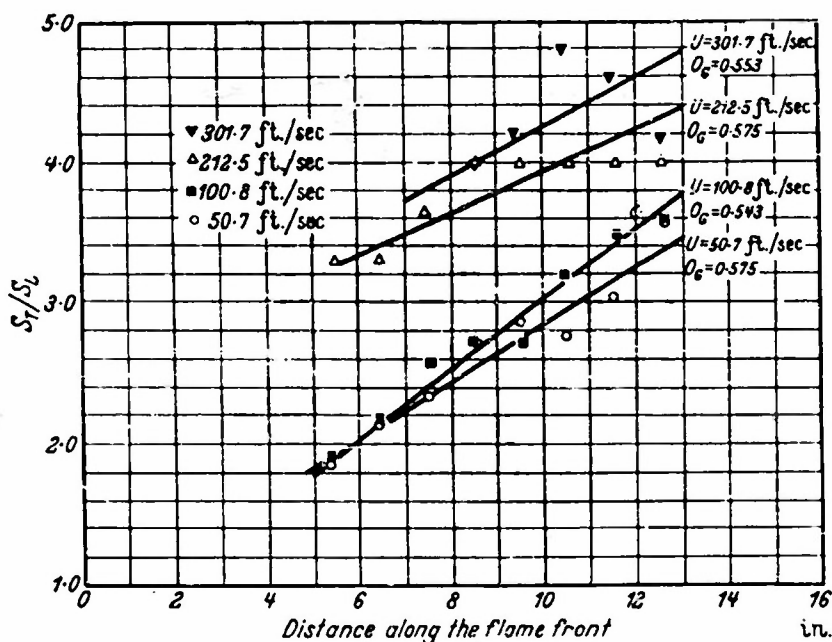


Fig. 9. Variation of S_T/S_L with distance from stabilizer for several flow velocities, after SCURLOCK²¹

* For example, most of the early results of DAMKÖHLER* with turbulent bunsen flames were so based.

determined from flame photographs. Their results may be expressed approximately in terms of tube diameter D , flow velocity U , and \bar{S}_T/S_L by the empirical relation:

$$\bar{S}_T/S_L = kD^{1/4}U^{1/4} \quad \dots (2)$$

where k is a constant of proportionality. Values of \bar{S}_T for the flow velocities employed are found to range up to about twice the laminar flame velocity.

Karlovitz, Denniston and Wells¹⁴ also studied open bunsen flames disturbed by pipe turbulence. Measurements of S_T/S_L versus distance from the burner tube center for stoichiometric natural gas-air and acetylene-air flames at several flow velocities and using a 3.16 cm tube are reported. These data are shown in *Fig. 6* as S_T/S_L versus distance from the tube center expressed in tube radii. S_T/S_L is observed to increase rapidly from near unity close to the tube rim, with the rate of increase becoming less rapid as distance from the tube rim increases. Values range up to above four and are higher at the higher flow velocities.

S_T at any point along the flame front was obtained from measurement of the sine of the included angle β between the tube axis and the mean position of the flame, as denoted by maximum brightness on flame photographs, by means of the relation $S_T = U \sin \beta$, where U is taken as the local flow velocity in the tube. Values of S_T determined in this way are incorrect to the extent that the flow of the unburned gases entering the flame front at a given distance from the burner rim differs from that in the tube. The pressure drop ΔP through any section of the flame brush is a direct function of the local value of S_T^* . Since S_T increases from the burner rim upward, the local pressure drop across the flame front also increases. Thus, since the static pressure on the burned gas side of the flame front is essentially atmospheric at all heights above the rim, the static pressure in the unburned gases must increase from the tube exit upward. This results in a reduction in velocity and a divergence of flow in the unburned gases which introduces an error of unknown magnitude in Karlovitz's results.

WOHL and his co-workers³³ have recently obtained data with bunsen flames disturbed both by pipe turbulence and by turbulence generated by grids placed near the tube outlet. Butane-air flames were studied over a range of mixture ratios and at different flow velocities. Data were taken using 2.55 cm and 1.01 cm tubes. Wohl determined the average flame velocity \bar{S}_T based on the mean flame surface taken as the surface of maximum luminosity on flame photographs. His results in the presence of pipe turbulence are therefore comparable to those of Bollinger and Williams. Plots of flow velocity versus \bar{S}_T as found by Wohl are shown in *Fig. 7*. The increase in \bar{S}_T with U is clearly shown. The effect of mixture ratio is shown in *Fig. 8*, where \bar{S}_T is plotted versus the generalized oxidant fraction, O_G , for several conditions of turbulence using the 2.55 cm tube. *Fig. 8(a)* is at a flow velocity of 540 cm/sec and *Fig. 8(b)* is at 1495 cm/sec. A substantial increase in \bar{S}_T with turbulence intensity is found, with maximum \bar{S}_T at the highest turbulence intensity and flow velocity ranging up to about four times the maximum value of S_L . A marked shift of the maximum further toward the rich side with increasing turbulence intensity is observed for these

* Actually, $\Delta P = \rho_u S_T^* \left(\frac{\rho_u}{\rho_b} - 1 \right)$



(a)

$U = 301.7 \text{ ft/sec}$
 $O_G = 0.553$
 Stabilizer diameter
 $= 0.038 \text{ in.}$
 from SCURLOCK²¹



(b)

$U = 232 \text{ ft/sec}$
 $O_G = 0.455$
 Stabilizer diameter
 $= 0.2 \text{ in.}$
 from WILLIAMS and SHIPMAN²⁸

Fig. 10. Photograph of flames stabilized in high-velocity flows in constant cross-section duct

butane-air flames, the maximum observed \bar{S}_T of 165 cm/sec which occurs with the four-mesh screen thus being found at $O_G = 0.42$ where S_L is less than 30 cm/sec ($\bar{S}_T/S_L \simeq 6.0$).

The foregoing results are for open flames. SCURLOCK^{21,22}, WILLIAMS, HOTTEL and SCURLOCK²⁷, and WOHL, SHORE, VON ROSENBERG and WEIL³³ have studied turbulent flames confined in constant-cross-section ducts. The original results are believed to be of only limited value because the upstream extremity of the flame brush was employed for determination of S_T . Re-analysis of some of these data using the mean flame front is, however, possible.

In Fig. 9, calculated from some of the flame photographs of Scurlock²¹, plots of the ratio of turbulent to laminar flame velocity S_T/S_L versus the distance from the stabilizer (measured along the flame front) are given under comparable conditions for lean Cambridge city gas-air flames confined in a 1×3 inch duct for several inlet velocities varying from about 50 to 300 ft/sec. Flames were stabilized in the wake of a 0.038-inch rod oriented normal to the flow and across the short dimension of the chamber. Gases entered the combustion chamber from a calming section through a nozzle. Turbulence in the gases approaching the combustion zone was thus below 0.5 per cent and the flow was uniform. Values of S_T are based on the mean flame position determined from maximum luminosity on the flame photographs*, and calculation of S_T is by the method developed by Scurlock²² which takes flow divergence of gases approaching the flame front into account.

The precision with which the location of any one point is determined is rather low (estimated to be about ± 0.5 ft/sec for S_T), but general trends of the data are unmistakable. The flame velocity tends toward higher values as flow velocity and distance downstream from the stabilizer increases. Maximum values of S_T range up to above four, being of the same order as those observed for unconfined flames.

Generation of turbulence in flames stabilized in ducts

Fig. 10(a) is one of Scurlock's²² photographs (0.4 second exposure) of a flame stabilized in a high-velocity stream at $U = 301.7$ ft/sec and $O_G = 0.553$. The extreme turbulence present in such a flame is revealed in Fig. 10(b) which is a spark Schlieren photograph of a similar flame from the paper by WILLIAMS and SHIPMAN²⁸.

In Fig. 11, flame width (reduced) of the mean flame front versus distance from the stabilizer is shown for the Fig. 10(a) flame. This curve has been extrapolated to the wall†. From these flame widths, a curve showing the increase in S_T/S_L with distance from the stabilizer has been computed (by the method of Scurlock²²) and is also included. S_T/S_L is estimated to rise to the remarkably high value of 17 near the wall. These high flame velocities could only be the result of high turbulence at the flame front and this is corroborated by the Fig. 10 photographs. Since the approach stream turbulence was known to be very low, the existence of turbulence must be

* The original values of S_T given by Scurlock²¹ were based on the upstream extremity of the flame instead of its mean position. Values obtained by the two methods vary roughly by a factor of two, those based on the outer extremity being, of course, the greater.

† Confidence in the approximate correctness of this extrapolation is enhanced by a knowledge of the chamber length necessary substantially to complete combustion.

attributed to the presence of the stabilizer, to generation of turbulence by the flame, or to both.

Scurlock²², and Williams, Hottel and Scurlock²⁷ have shown how turbulence can be generated in such a flame and have obtained experimental and theoretical results which are believed to document adequately their explanation. Flow in the vicinity of the combustion zone is shown schematically in Fig. 12. Immediately downstream from the stabilizer, high velocity gradients exist across the flame front between the fast-flowing unburned gases and the relatively slow-moving burned gases in the eddy region to the rear of the stabilizer. Such gradients are under certain conditions responsible for generating a high level of turbulence which results in the observed high local rates of combustion. Just downstream of the eddy region the mean velocity of the burned gases is much lower than that of the adjacent stream of unburned mixture. Under the influence of the large pressure drop resulting from the combustion process, however, the slow-

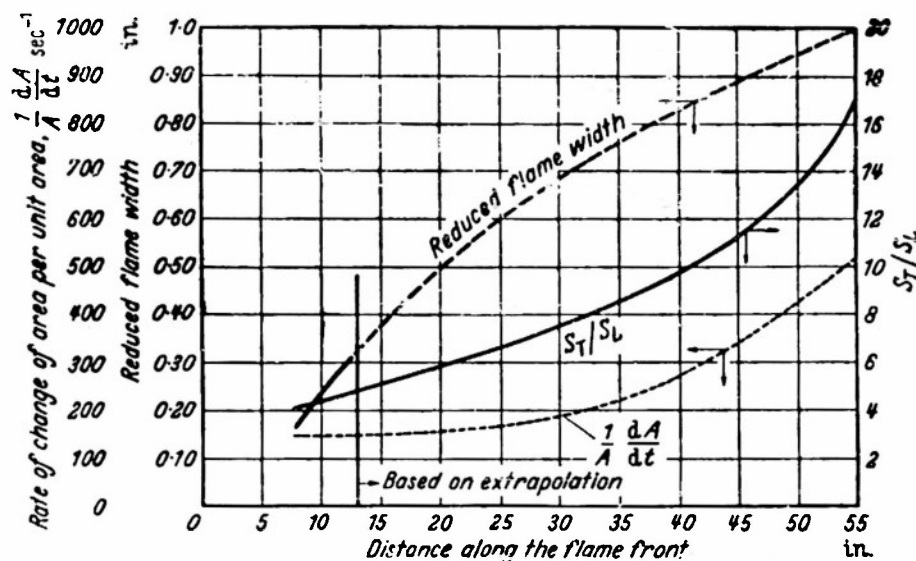


Fig. 11. Flame width, St/St_L , and $\frac{1}{A} \frac{dA}{dt}$ versus distance from stabilizer for Fig. 10(a) flame extrapolated to wall

moving low-density burned gases accelerate more rapidly than does the unburned mixture until their velocity equals, and finally exceeds, that of the adjacent unburned gases. In the region where the velocity of the burned gases approximates that of the main stream, generation of little new turbulence would be expected, although that previously in existence would maintain a high rate of combustion. As velocity gradients are again created by the greater acceleration of the burned gases, additional turbulence may under suitable conditions be generated and the rate of combustion continue to increase.

The amount of turbulence generated in the region immediately downstream of the flame stabilizer increases rapidly with stream velocity. Turbulence generation in this region depends, however, not only on the magnitude of the velocity gradients but also on the distance over which the gradients

exist. Larger flame stabilizers thus tend to encourage turbulence generation. Since the rate of increase in relative velocity of the burned gases from their low-velocity just downstream of the eddy region is a direct function of the pressure drop in the duct which is in turn a direct function of the rate of increase of gas volume, the higher the rate of volume increase in this region the shorter the distance over which velocity gradients exist and thus the smaller the turbulence generation. An increase in flame temperature or flame speed would, therefore, be expected to tend to suppress the generation of turbulence in this region.

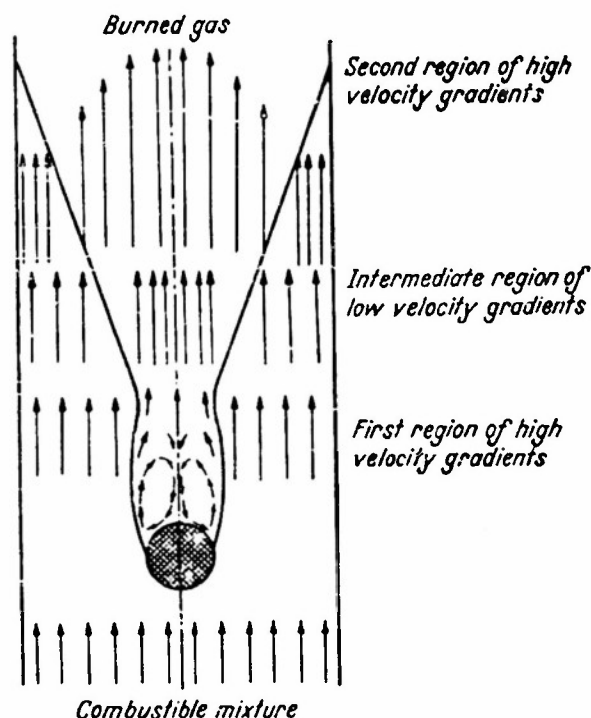


Fig. 12. Schematic diagram of flow in vicinity of combustion zone for flame stabilized in a constant cross-section duct, after SCURLOCK²²

The effects of flame velocity and flame temperature are opposite in the second region of high velocity gradients further downstream where the hot combustion products move at a higher velocity than the unburned mixture, since faster burning and higher temperature result in higher velocity gradients. An increase in stream velocity, however, tends to increase the turbulence in this region just as in the first region.

Although the first region of velocity gradients is associated with the presence of the stabilizer and turbulence generation is greatly influenced by stabilizer size and shape, the existence of the second region of gradients is independent of the stabilizer, and turbulence produced in this region is truly flame generated.

Discussion of Theory

Gerhard DAMKÖHLER⁵ was the first important worker to study quantitatively the effects of turbulence on flames. He postulated a basic distinction

between the effects of turbulence on the flame depending upon whether the turbulence scale was very large or very small relative to the thickness of the laminar flame front.

For a turbulence scale very small relative to the laminar flame front thickness, it was proposed that the only effect of turbulence was to increase the flame velocity by increasing the transport of heat and active species by eddy diffusion. SHELKIN²⁴ concurred in this view, and on the assumption that transfer of heat was the controlling factor in determining flame velocity proposed the following relation:

$$\frac{S_T}{S_L} = \sqrt{\frac{\epsilon + \kappa}{\kappa}} \quad \dots (3)$$

where ϵ is the eddy diffusivity and κ is the thermal diffusivity. Present workers are tentatively willing to accept this picture although experimentally no flames disturbed by turbulence of a scale very small relative to the flame front have ever been investigated; and, in fact, such a situation would in practice be very unlikely. Perhaps, however, at very low pressures where the flame front thickness is greatly increased such a situation could be obtained and would probably be worthy of study.

For a turbulence scale very large relative to the laminar flame front thickness, the situation which appears on the basis of experimental evidence to correspond most closely to that generally encountered in practice, Damk hler concluded that the observed increase in burning rate is due only to wrinkling of the flame surface. Embodiment of this picture in a quantitative relation expressing S_T in terms of the parameters of the turbulence and the flame was early recognized to be of importance and has received attention from several workers. Thought was hampered, however, for a number of years by failure to recognize (a) the statistical nature of the flame distortion by turbulence, and (b) the importance of time under all practical conditions in determining the extent of flame distortion. Karlovitz *et al*¹⁴ have made important contributions to this problem, and SCURLOCK and GROVER²⁵ have recently published work which, while still subject to refinement, is believed to embody the principal necessary elements of a quantitative theory.

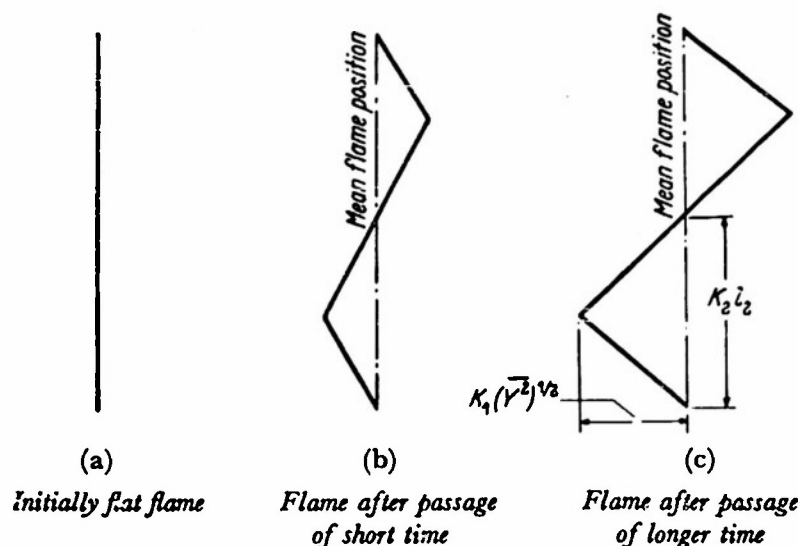
Scurlock and Grover in their development consider an initially flat flame of infinite extent oriented normal to the y -axis propagating into a combustible mixture agitated by isotropic turbulence with an intensity v' ($= u' = w'$) and scales l_1 and l_2 defined in the Lagrangian and Eulerian manner respectively. Only turbulence with a scale very large compared with the thickness of the laminar flame front is considered, the turbulence being assumed only to wrinkle and extend the flame surface, the laminar flame velocity remaining constant and unaffected by any increase in transport properties or by flame curvature. As time passes, the flame becomes wrinkled by eddy diffusion of flame elements away from the mean position of the flame, and the flame area is increased as shown schematically in Fig. 13. Assuming, as indicated in Fig. 13(c), that the depth of the wrinkles is proportional to the root-mean-square displacement of a flame element from the mean flame front, $(\bar{r}^2)^{\frac{1}{2}}$ or equal to $K_1(\bar{r}^2)^{\frac{1}{2}}$, where K_1 is a proportionality constant, and that the

average base width of these wrinkles is proportional to l_2 , or equal to $K_2 l_2$ where K_2 is a second constant of proportionality, the following relation for the ratio of wrinkled to initially flat flame area A_T/A_L is obtained from simple geometric considerations:

$$\frac{A_T}{A_L} = \frac{S_T}{S_L} = \left[1 + c_1 \left(\frac{\bar{Y}^2}{l_2^2} \right) \right]^{\frac{1}{2}} \quad \dots \quad (4)$$

where $4K_1^2/K_2^2$ has been replaced by the constant c_1 .

As time passes and the initially flat flame becomes wrinkled, three effects are believed to be of importance in determining \bar{Y}^2 and thus the flame area: (1) eddy diffusion associated with the turbulence present in the flame, (2) flame propagation, and (3) flame-generated disturbances.



$$\frac{S_T}{S_L} = \frac{A_T}{A_L} = \frac{\left\{ \left[\frac{1}{2} K_2 l_2 \right]^2 + \left[K_1 (\bar{Y}^2)^{\frac{1}{2}} \right]^2 \right\}^{\frac{1}{2}}}{\frac{1}{2} K_2 l_2} = \left[1 + \frac{c_1 \bar{Y}^2}{l_2^2} \right]^{\frac{1}{2}}$$

Fig. 13. Schematic diagram showing wrinkling with passage of time of an initially flat flame element exposed to turbulence²⁵

Eddy diffusion tends to increase \bar{Y}^2 and thus the flame area without bound with time. Under the hypothetical conditions where the flame propagates at a very low velocity so that v'/S_L is very large (thus eliminating the second effect) and no change in density occurs upon passage of gases through the flame front (thus eliminating the third effect), TAYLOR's²⁵ theory of diffusion by continuous movements applies to diffusion of flame elements in the field of turbulence and yields the following relation between \bar{Y}^2 , v' , and time t :

$$\frac{d(\bar{Y}^2)}{dt} = 2 v'^2 \int_0^t R_t dt \quad \dots \quad (5)$$

where R_t is the correlation coefficient defined as the mean value of the product of the fluctuating velocity in the y -direction of a fluid particle, in this case coinciding with a flame element, at zero time and the fluctuating

velocity of the same fluid particle at time t , divided by the mean square fluctuating velocity of the particle.

Removal of the restriction that v'/S_L is very large requires modification of Eq. (5). In the absence of flame propagation the correlation coefficient R_t may be employed, because the assumption is valid that a diffusing flame element is bound during the diffusion process to a single fluid particle. If the flame propagates during diffusion, the fluctuating velocity of a single flame element is affected not only by passage of time but by its movement from one fluid particle to another as the burning process proceeds. A mixed correlation coefficient R_y which takes into account flame propagation must thus be defined for use in Eq. (5) which measures the correlation between the fluctuating velocity of a flame element at zero time and that of the same flame element at a later time after the flame has propagated into the unburned gas a distance $y = S_L t$. R_y may be represented as the product of the correlation coefficient R_t expressing the correlation of the fluctuating velocities of single fluid particles at zero time and after passage of the time t , and the correlation coefficient R_y expressing the correlation of the fluctuating velocities at the same time of fluid particles separated by a distance y .

Eq. (5) thus becomes

$$\frac{d(\overline{\gamma^2})}{dt} = 2 v'^2 \int_0^t R_y dt = 2 v'^2 \int_0^t R_t R_y dt \quad \dots (6)$$

Recalling Taylor's definition of Lagrangian scale, $l_1 \equiv v' \int_0^\infty R_t dt$ and Eulerian scale, $l_2 \equiv \int_0^\infty R_y dy$, and accepting after Dryden⁶ the approximations $R_t = \exp -v't/l_1$ and $R_y = \exp -S_L t/l_2$, Eq. (6) becomes

$$\begin{aligned} \frac{d(\overline{\gamma^2})}{dt} &= 2 v'^2 \int_0^t \exp -\left(\frac{v'}{l_1} + \frac{S_L}{l_2}\right) t dt = 2 v'^2 \left(\frac{1}{\frac{v'}{l_1} + \frac{S_L}{l_2}} \right) \\ &\times \left[1 - \exp -\left(\frac{v'}{l_1} + \frac{S_L}{l_2}\right) t \right] \quad \dots (7) \end{aligned}$$

Replacing l_1 by the more easily measurable l_2 by assuming on the basis of TAYLOR'S²⁴ discussion of data for turbulence behind grids that $l_1 \simeq \frac{1}{2} l_2$ and putting in dimensionless form in terms of a reduced displacement $(\overline{\gamma^2})^{1/2}/l_2$, a reduced turbulence intensity v'/S_L , and a reduced time $S_L t/l_2$, Eq. (7) may be rewritten as follows:

$$\frac{d \left[\frac{(\overline{\gamma^2})^{1/2}}{l_2} \right]}{d \left[\frac{S_L t}{l_2} \right]} = \frac{v'}{S_L} \frac{1 - \exp \left(-\frac{v'}{S_L} \right) \left(2 + \frac{S_L}{v'} \right) \left(\frac{S_L t}{l_2} \right)}{\frac{(\overline{\gamma^2})^{1/2}}{l_2} \left(2 + \frac{S_L}{v'} \right)} \quad \dots (8)$$

Integration yields

$$\frac{\overline{\gamma^2}}{l_2^2} = \frac{2 \left(\frac{v'}{S_L} \right) \left(\frac{S_L t}{l_2} \right)}{2 + (S_L/v')} \left\{ 1 - \frac{\left(\frac{S_L}{v'} \right) \left(\frac{l_2}{S_L t} \right)}{2 + (S_L/v')} \left[1 - \exp \left(-\frac{v'}{S_L} \right) \left(\frac{S_L t}{l_2} \right) \left(2 + \frac{S_L}{v'} \right) \right] \right\} \quad \dots (9)$$



(a)
 $S_L = 33 \text{ cm/sec}$
 $O_a = 0.515$
 Turbulence intensity
 $= 0.8\%$



(b)
 $S_L = 25 \text{ cm/sec}$
 $O_a = 0.547$
 Pipe turbulence
 Turbulence intensity
 $= 5.3\%$



(c)
 $S_L = 25 \text{ cm/sec}$
 $O_a = 0.547$
 Turbulence intensity
 $= 7.5\%$

Fig. 14. Spark Schlieren photographs of turbulent burner flames (methane-air) after Wohl³⁰, showing (a) increase in flame wrinkling with distance from burner rim, (b) increase in wrinkling with increase in turbulence intensity, and (c) sharp flame edges protruding into the burned gases and curved surfaces extending into the unburned mixture

The importance of time of exposure to the turbulence in determining \bar{Y}^2 is clearly indicated. On the basis of these relations, it may be concluded that eddy diffusion, in the absence of other effects, would continue to increase \bar{Y}^2 , and thus the flame area and S_T/S_L without bound with time, the rate of area increase being made greater by increasing v' by decreasing S_L , and by decreasing l_s .

In order to apply these relations to a real situation such as a flame stabilized on the rim of a burner tube where the flame is oriented obliquely to the flow of unburned gases and a component of velocity exists normal to the flame front, it is necessary to know not only S_L , v' , and l_s , but also the time of exposure of any small segment of the mean flame to the turbulence. If β is the included angle between the direction of flow of unburned gases and the mean flame front and U is the local flow velocity, initially flat flame segments generated at the rim move along the flame front with a velocity $U \cos \beta$ until they disappear upon reaching the wall or upon intersecting another flame front. The time of exposure of any flame segment to the turbulence may be expressed as $t = \int_0^L (dL/U \cos \beta)$ where L is the distance measured along the mean flame front from the burner rim to the flame segment under consideration. It would thus be expected on the basis of the above relations that for a turbulent bunsen flame, or any other flame extending downstream from a stabilizer and disturbed by turbulence, that a thickening of the turbulent flame brush and an increase in flame wrinkling would occur as L increases. This conforms with experimental observations of turbulent flames and is clearly indicated in the dark Schlieren photographs of WOHL and SHORE³⁰ shown in Fig. 14.

The tendency for flame propagation to flatten and decrease the surface of a turbulent flame was first pointed out by Karlovitz, Denniston, and Wells¹⁴. This effect is demonstrated schematically in Fig. 15 where a wrinkled flame no longer disturbed by turbulence is propagating into stagnant unburned gas. It is further assumed that no change in gas density occurs due to combustion, which eliminates motion in the unburned gas due to approach of the flame. The flame has propagated in the time interval dt from its initial position represented by the solid line to the new position represented by the broken line; and as demonstrated by Karlovitz, the flame area has clearly been reduced by propagation with sharp edges now only protruding into the burned gases and curved surface elements extending into the unburned mixture. This corresponds to the appearance of actual turbulent flames such as those shown in Fig. 14.

Again representing the distance from the mean flame position to the mean apex of the protrusions by $K_1(\bar{Y}^2)^{1/2}$, the distance in the y -direction from the apex of the protrusion into the burned gas to that into the unburned gas is $2K_1(\bar{Y}^2)^{1/2}$. The rate of change of this quantity due to propagation consists of two terms, a positive term representing the increase at the apex of the protrusion into the unburned gas which equals S_L , and a negative term representing a decrease at the apex of the protrusion into the burned gas which geometric considerations reveal to be $-S_L[1 + c_1(\bar{Y}^2/l_s^2)]^{1/2}$. By combining these terms, rearranging, and replacing $\frac{1}{2}K_1$ by the constant c_2 ,

Fig. 16 is helpful in enabling one to visualize the effects of eddy diffusion and flame propagation acting together on a flame extending downstream from a stabilizer. The distortion of such flames upon passage of single

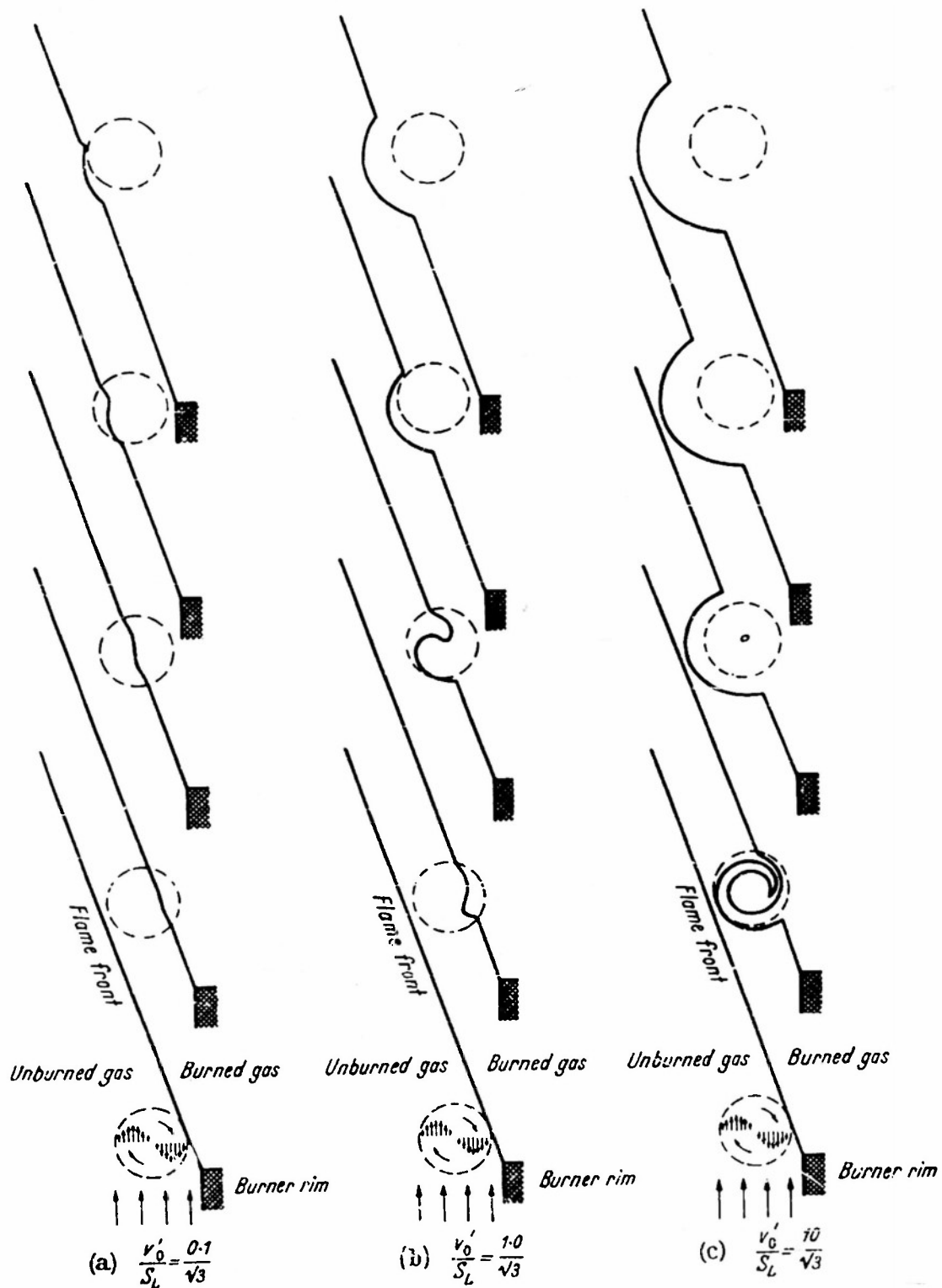


Fig. 16. Distortion of stabilized flames during passage of single eddies

turbulent eddies of a specialized nature has been graphically determined for cases corresponding to several values of v'/S_L . The two-dimensional disturbing eddy is assumed to be in rotary motion with the intensity of

velocity components superimposed on the mean flow along any diameter corresponding to a sine wave, the center and outer extremities of the eddy moving at stream velocity as indicated. The root-mean-square value of these superimposed velocities averaged along any diameter equals $\sqrt{3v'}$, the component of superimposed velocity in one direction averaged over the

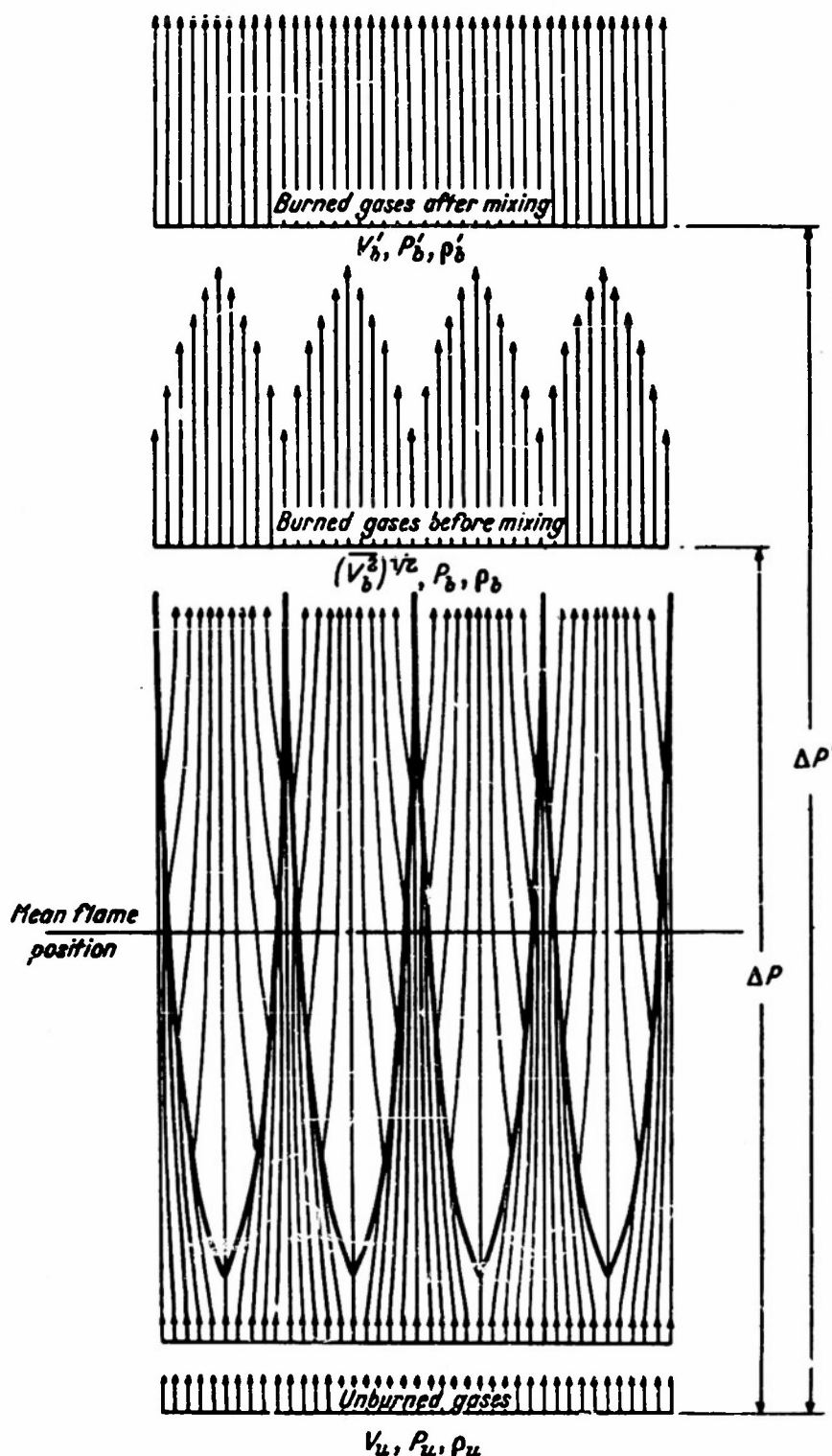


Fig. 17. Flow pattern in neighborhood of wrinkled flame element constructed in accordance with SCURLOCK's calculations²² for $\rho_u/\rho_b = 6$

entire eddy thus equaling v' . The considerable effect of v'/S_L on the degree of flame distortion, the initial increase in the distortion with time, and the movement of the distortion downstream away from the stabilizer with time are all clearly shown. The growth and movement downstream of flame distortions caused by single eddies similar to those shown in Fig. 16 were observed experimentally by MARKSTEIN¹⁹ with an open bunsen flame stabilized on the rim of a rectangular tube. Markstein, however, interpreted the growth of the distortions with movement downstream as evidence of the presence of flame-generated turbulence.

Flame-generated disturbances may be produced by velocity gradients induced by the pressure drop across the combustion zone associated with the density decrease of the gases upon passage through the flame front, and in most instances are believed to be of importance in distorting the flame. The work of Scurlock^{22, 27} establishing the existence and importance of this effect for confined flames has already been discussed.

The effect is demonstrated in Fig. 17 where the two-dimensional flow pattern in the vicinity of a wrinkled flame element has been constructed on the basis of Scurlock's steady-state flow calculations for $\rho_u/\rho_b = 6$, where ρ_u and ρ_b are the densities of the unburned mixture and of the burned gases respectively. The combustion pressure drop causes the low-density burned gases to accelerate more rapidly than the unburned gases. The uniform flow is thus converted upon passage through the combustion zone into a non-uniform flow with large velocity gradients. These gradients are a potential source of turbulence and under conditions where the Reynolds number of the flow is sufficiently high, all of the energy decrease resulting from mixing of the gases issuing from the combustion zone might conceivably appear in the form of turbulence. Such flame-generated turbulence would be available for further distortion of the flame by eddy diffusion.

The following relation for this maximum energy available for turbulence generation E_m has been derived by Scurlock and Grover by combination of a momentum balance between the unburned gases and gases issuing in non-uniform flow from the combustion zone, and a mass balance and momentum balance between the unburned gases and gases issuing in uniform flow from the combustion zone after complete mixing :

$$E_m = \frac{K}{2} \frac{\rho_u V_u^3}{\rho_b} \left(\frac{\rho_u}{\rho_b} - 1 \right) \quad \dots (12)$$

where V_u is the approach velocity of the unburned gases normal to the mean flame front and $K = [(\Delta P/\Delta P') - 1]$ where $\Delta P/\Delta P'$ is the ratio of pressure drops between the unburned and burned unmixed gases and unburned and burned mixed gases. Scurlock and Grover have given calculated maximum values of K designated K_m for $S_T/S_L = \infty$. Values of K_m in the range of prime interest— ρ_u/ρ_b from about four to ten—were found to equal approximately $\rho_u/100\rho_b$, and the following approximate final relation was suggested for E_m :

$$E_m \simeq \frac{K_m}{2} \left(\frac{\rho_u}{\rho_b} \right) (V_u^3 - S_L^3) \left(\frac{\rho_u}{\rho_b} - 1 \right) \quad \dots (13)$$

TURBULENT COMBUSTION

Assuming isotropy of the generated turbulence, E_m is related to the maximum turbulence intensity that could result from the third effect v_m' as follows :

$$E_m = \frac{3v_m'^2}{2} \quad \dots (14)$$

Solving for v_m' and substituting for E_m its approximate value from Eq. (13),

$$v_m' = \left(\frac{2E_m}{3} \right)^{\frac{1}{2}} \simeq \left[\frac{K_m}{3} \left(\frac{\rho_u}{\rho_b} \right) (V_u^2 - S_L^2) \left(\frac{\rho_u}{\rho_b} - 1 \right) \right]^{\frac{1}{2}} \dots (15)$$

Thus in instances where $V_u^2 \gg S_L^2$ the maximum turbulence intensity that could be generated increases approximately as the first power of V_u and as the three-halves power of ρ_u/ρ_b .

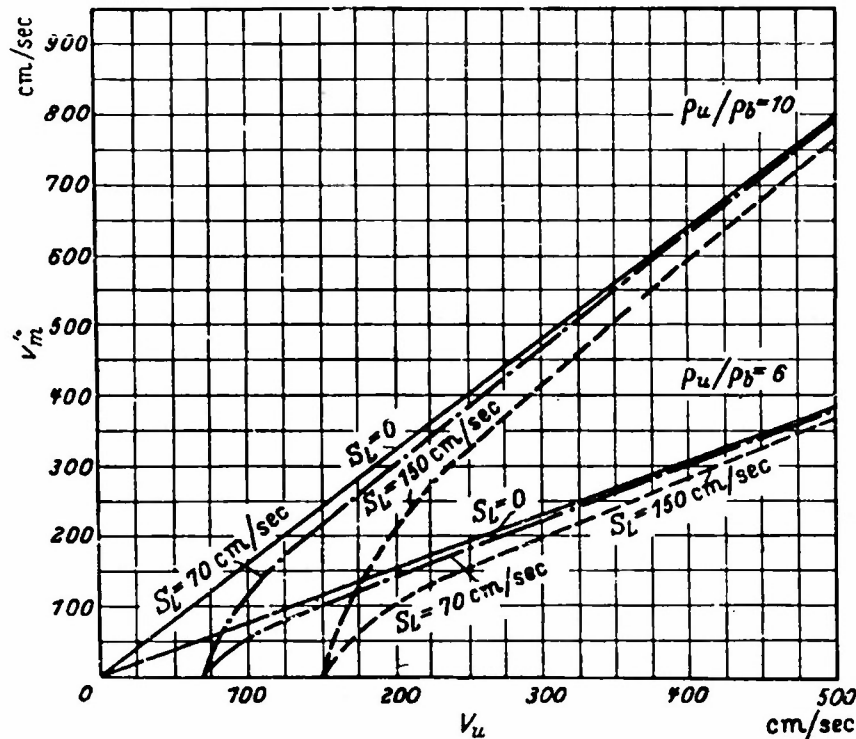


Fig. 18. Maximum possible flame-generated turbulence under various conditions of V_u , ρ_u/ρ_b and S_L in accordance with Eq. 15

Eqs. (13) and (15) may be applied either to open flames or to flames confined in ducts. With unconfined flames, V_u is the normal velocity of the unburned gases relative to the mean flame front, thus equaling S_T . For confined flames, V_u is the normal flow velocity relative to the confined combustion zone, which generally corresponds to the flow velocity in the duct and would in most instances be much greater than S_T of the oblique flame fronts. Several solutions of Eq. (15) are given as plots of v_m' versus V_u , as shown in Fig. 18. These maximum turbulence intensities are observed to be of the same order as V_u . The discovery by Scurlock that the effect of approach turbulence on confined flames stabilized in high-velocity flows is generally unimportant compared with that due to flame-generated disturbances is not surprising in the light of Eq. (15), and would be expected for such flames even if only a small fraction of the available energy were

converted to turbulence. For open flames where $V_u = S_T$, the situation in practical instances is such that both the approach turbulence and that generated in the flame might be expected to play important roles.

The above theoretical discussion of the effects of flame-generated turbulence was limited to the conversion of available energy to isotropic turbulence. In view of the mechanism of turbulence generation at regions of shear between fluid streams, which first requires the development of instability followed by formation of a more or less systematic eddy street, it is likely that turbulence generated in the wrinkled flame is far from isotropic. What effect this probable absence of isotropy has on the previous discussion is not known and remains to be determined by experiment.

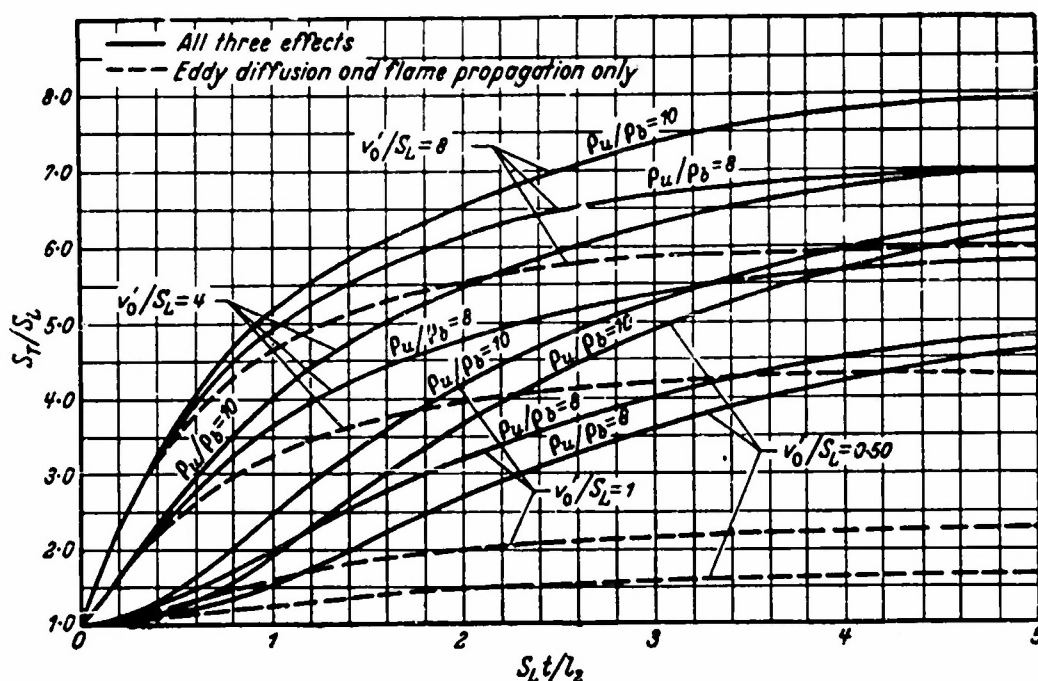


Fig. 19. S_T/S_L versus $S_L t/l_2$ calculated for several different conditions taking into account eddy diffusion, flame propagation, and flame-generated turbulence²³

Solutions of Eq (11) have been obtained by Scurlock and Grover by a trial-and-error stepwise method for *open flames* taking into account eddy diffusion, flame propagation, and flame-generated turbulence for a range of values of v'_0/S_L , where v'_0 is the turbulence intensity in the approach stream and for ρ_u/ρ_b of eight and ten, and these solutions have been combined with Eq. (4). The results are shown in Fig. 19 as plots of S_T/S_L versus $S_L t/l_2$. For the purpose of these calculations, it was assumed that 100 per cent of the available energy was transformed into turbulence in accordance with Eq. (15), and that the scale of the generated turbulence is the same as that of the approach stream. Flame-generated turbulence intensity determined from Eq. (15) was combined with that in the approach stream, v'_0 , by means of the relation $v' = \sqrt{(v'_0)^2 + (v'_m)^2}$ to obtain a v' for use in Eq. (11). Both K_1 and K_2 were assigned the values of 2^* , thus making $c_1 = 4$ and $c_2 = 1/4$.

* This is in approximate agreement with the measurements of turbulent flame wrinkles made by HOTTEL, WILLIAMS and LEVINE¹¹ on the basis of which K_2 would probably be assigned a value of 2.5. Assignment of a value of 2 to K_1 would appear to be a reasonable approximation on the basis of geometric considerations.

Assuming that these curves cover the S_L/l_2 range of practical interest, it is indicated that turbulent flame segments generally do not reach an equilibrium condition of constant flame area but are continuing to increase in area when their short existence ends either at a wall or upon intersecting another flame front.

Several solutions taking into account eddy diffusion and flame propagation only are included for comparison as the broken curves in Fig. 19. Considered as a percentage, the effect of flame-generated turbulence is indicated to be of much less importance at high values of v_0'/S_L .

Fig. 20 demonstrates individually the effect of eddy diffusion, flame propagation, and flame-generated turbulence predicted by the theory for a

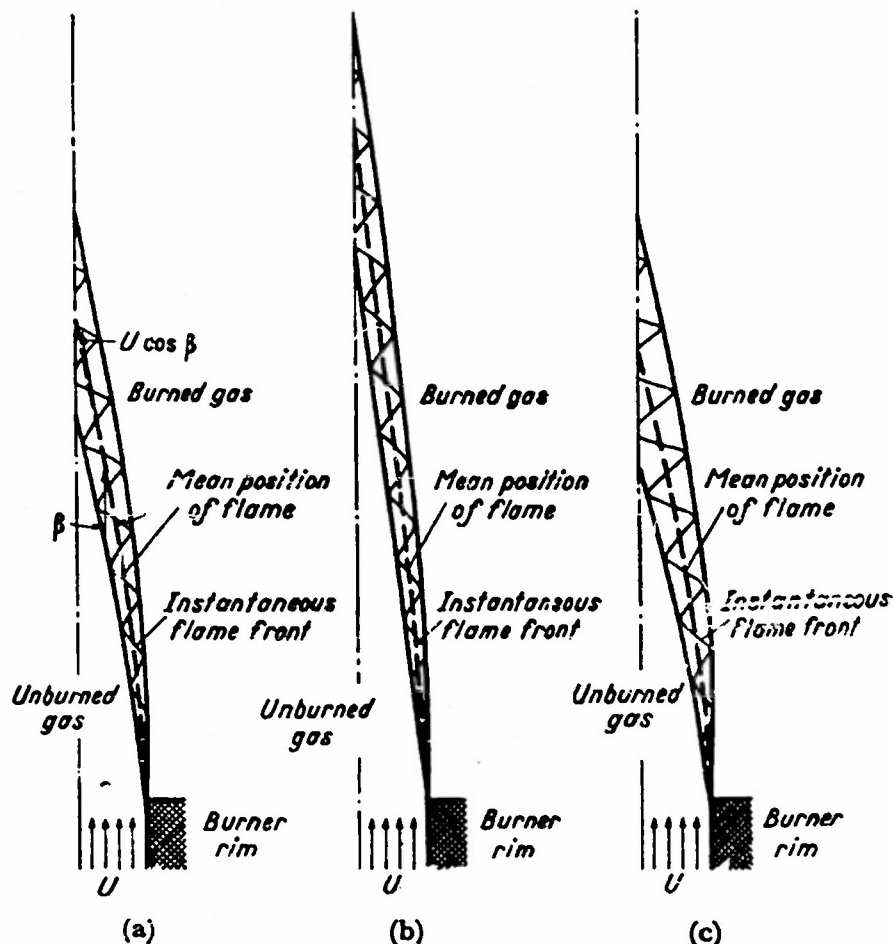


Fig. 20. Cross section of stabilized unconfined bunsen flames constructed on basis of theory²² to demonstrate under typical conditions the predicted individual effects of eddy diffusion, flame propagation, and flame-generated turbulence (assumed conditions: $S_L = 10$ cm/sec, $U = 200$ cm/sec, 5 per cent turbulence intensity, $D = 5$ cm, $l_2 = 0.25$ cm, flame brush half width = $2(\overline{T^2})^{1/2}$)

typical open bunsen flame. Assuming $S_L = 10$ cm/sec, $v = 200$ cm/sec, a 5 per cent turbulence intensity [$v_0'/S_L = (200 \times 0.05)/10 = 1$], a uniform flow velocity, $D = 5$ cm, $l_2 = 0.25$ cm, and a flame-brush width of $2(\overline{T^2})^{1/2}$, Fig. 20(a) has been constructed on the basis of Eq. (8), which takes into account eddy diffusion only, and Eq. (4). The effect of addition of the term taking into account flame propagation is shown in Fig. 20(b). A reduction in flame thickness, a decrease in S_T (as denoted by a smaller β) at a given distance

downstream from the stabilizer, and the tendency of the flame thickness to approach a constant value as distance from the stabilizer becomes large is noted. The effect of adding flame-generated turbulence to the other two effects is shown in *Fig. 20(c)* and is observed to cause an increased flame thickness and flame velocity.

Comparison of theory with experiment

Let us now compare the experimental results with those predicted by the relations of Scurlock and Grover.

Shown in *Fig. 21* as the solid lines are turbulent flame velocities computed under conditions similar to those present in the experiments of Bollinger and Williams. Values of \bar{S}_T for S_L of 40, 70 and 150 cm/sec, corresponding approximately to the flame velocities encountered by Bollinger and Williams for propane, ethylene, and acetylene, are plotted versus U . v_0' was taken as $0.05U$ and l_s as $0.05D$ for these computations—values considered

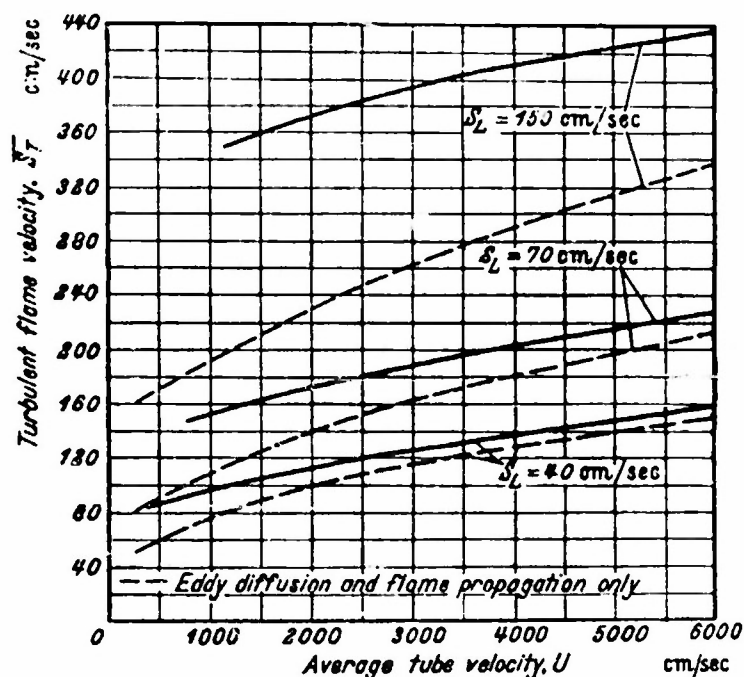


Fig. 21. Flame velocity calculated under conditions studied by BOLLINGER and WILLIAMS (approach stream v_0' taken as $0.05U$ and l_s taken as $0.05D$)

reasonable averages for fully-developed pipe turbulence—and the gases were assumed to issue from the tube at uniform velocity. ρ_u/ρ_b for the propane-air and ethylene-air flames was taken as eight, and for acetylene-air flames was taken as ten. Similar results taking into account only eddy diffusion and flame propagation are shown as the broken curves. These curves are included because of the inadequacy of the Scurlock and Grover relations in predicting how much of the maximum available flame-generated turbulence is actually effective in disturbing the flame. These calculated curves may be compared with the experimental results of Bollinger and Williams given in *Fig. 5*. Although the calculated and experimental curves are roughly similar, and the relation between \bar{S}_T and S_L seems to be about the same in both cases, the strong effect of scale (actually diameter) appearing in the experimental data is absent from the calculated results. Further, except for the largest burner tube, the calculated curves lie above the experimental results.

Two explanations have been advanced for this discrepancy²³. The first is that percentage conversion of available energy to turbulence may be strongly influenced by turbulence scale and thus, in turn, tube diameter. This was suggested by Scurlock's²² studies of stabilized flames wrinkled by flame-generated turbulence where it was found that under conditions favorable to the appearance of flame-generated disturbances*, the effective chamber width associated with the stabilized flame, which corresponds to a sort of scale, had a noticeable effect on the reduced flame width. It was reasoned that conditions favorable to the conversion of available energy to turbulence are those which increase the velocity difference between the burned and unburned gases and increase the distance along which the burned and unburned gas streams are adjacent. The velocity gradient tends to be increased by increasing V_u/S_L , increasing $[(\rho_u/\rho_b) - 1]$, and increasing V_u . The distance along which burned and unburned gases are adjacent would tend to be increased by increasing the scale l_2 .

Although these parameters, which may be combined with the kinematic viscosity ν to yield a sort of 'flame Reynolds number'

$$\frac{V_u l_2}{\nu} \left(\frac{\rho_u}{\rho_b} - 1 \right) \left(\frac{V_u}{S_L} \right)$$

undoubtedly are of importance in controlling the conversion of available energy to turbulence, preliminary calculations²³ have indicated that the effect of turbulence scale in the flame (assuming its proportionality to tube diameter) on this conversion is insufficient to account for the 0.5 power effect of tube diameter on \bar{S}_T found by Bollinger and Williams.

The second proposed explanation for the discrepancy is the postulated presence of a strong effect of flame curvature. This is considered by the present authors to be the more plausible explanation, although changes with tube diameter in percentage conversion of available energy to turbulence would certainly be expected to occur. Qualitatively, the effect of flame curvature under the mixture ratio conditions studied would be a tendency to flatten the flame, the effect being similar to that existing at the tip of a bunsen cone. Curvature would be greater at smaller scales and the effect increased, which could explain the lower values of \bar{S}_T with the smaller diameter burner tubes.

The experimental results of Karlovitz are compared with curves obtained from the theoretical relations in the five plots of Fig. 22. The solid curves are those obtained from solution of the theoretical relations assuming a five per cent mean turbulence level in the approach stream, uniform flow, and $l_2 = 0.05D$. The broken curves are calculated taking into account eddy diffusion and flame propagation only. The chain-dotted curves are the experimental results of Karlovitz shown previously in Fig. 6. Agreement between calculated and experimental results in view of the several uncertainties involved† is considered acceptable. In general the experimental values of S_T/S_L for natural gas-air flames fall between the two calculated curves while those for acetylene fall slightly above the calculated curves. This

* Disturbances generated in Scurlock's second region of instability (see Fig. 12) correspond to the flame-generated disturbances of interest here.

† Principal of these are (a) unknown effect of flow divergence in the unburned gases on the Karlovitz results, (b) difference in assumed and actual flow and turbulence conditions, (c) uncertainty about assignment of values to K_1 and K_2 , and (d) uncertainties about the actual effect of flame-generated disturbances previously discussed.

might be explained as resulting from a smaller effect of flame curvature with acetylene-air flames because of the smaller thickness of its laminar flame front.

Some of Wohl's experimental results for butane-air flames are compared with theoretical curves in the five plots of Fig. 23, where \bar{S}_T is plotted versus O_G . The theoretical curves taking into account all three effects are again represented as the solid lines, those taking into account eddy diffusion and flame propagation only as the broken lines, and the experimental results as the chain-dotted lines. For computing the theoretical curves the turbulence intensities used were those given by Wohl. The turbulence scale for pipe

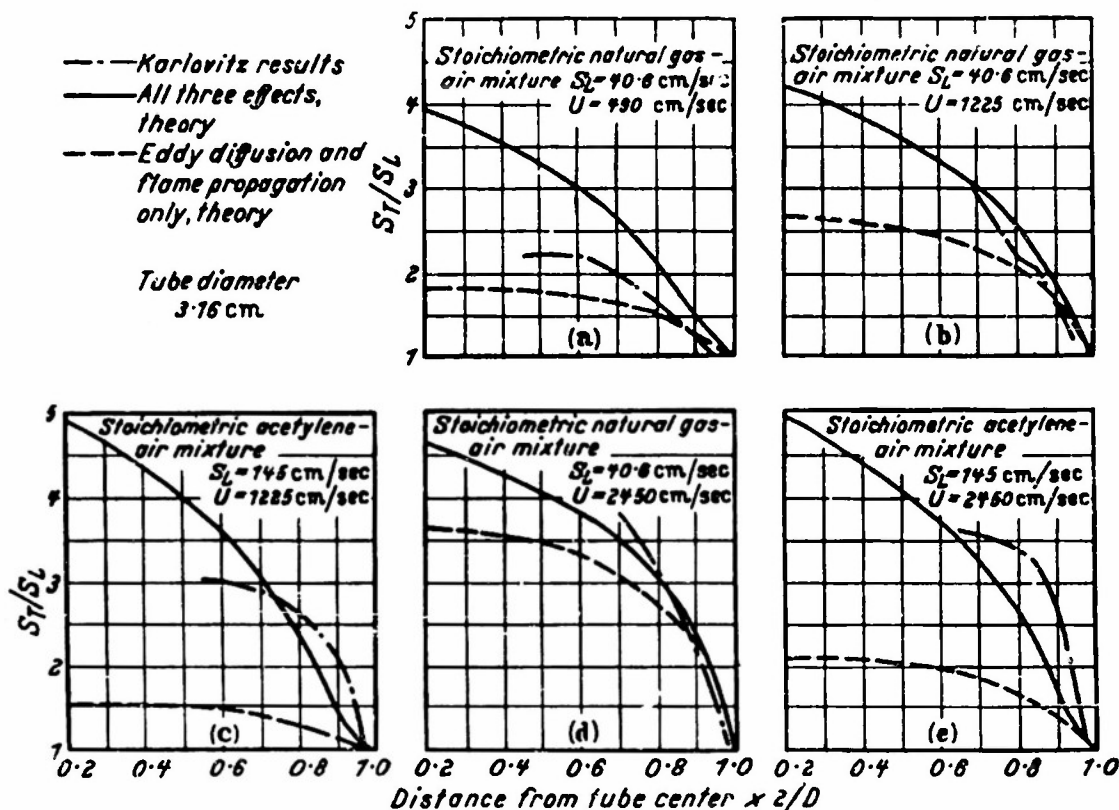


Fig. 22. Experimental results of KARLOVITZ, DENNISTON, and WELLS¹⁴ compared with theory (approach stream v_0' taken as $0.05U$ assumed uniform ρ_u/ρ_b taken as 8 for natural gas flames and 10 for acetylene flames)

turbulence was taken as equal to $0.05D$. For determining the scale where grids were used, the empirical relation suggested by DRYDEN⁸ was employed. Scale in the flame, when the 100-mesh screen was used, was assumed to be that at one inch downstream from the tube exit. For the ten- and four-mesh screens which were situated closer than 80 wire diameters from the tube exit, the scale was taken as that predicted at 80 wire diameters by Dryden's relation. With the exception of Fig. 23(c) for the 100-mesh screen and Fig. 23(e) for the four-mesh screen, the theoretical and experimental curves are of similar shape and height. As already noted in the discussion of Fig. 8, however, the experimental curves are all shifted toward the rich side. The lower than predicted experimental flame velocities with the 100-mesh screen [Fig. 23(c)] can perhaps be attributed to the small scale of the turbulence present. This could result in a low 'flame Reynolds number' and thus a

low conversion of available energy to turbulence. Flame curvature effects also might be expected under these conditions to tend to reduce flame area. The discrepancy between the experimental and theoretical curves with the four-mesh screen might be attributable to the lack of isotropy of the approach stream turbulence. The turbulence-generating grid was situated only about 19 wire diameters from the tube exit, whereas Dryden⁶ suggested that isotropy should not be assumed at distances from the grid less than about 80 wire diameters. A still more likely explanation for the anomalous position of this curve, however, is developed in the following discussion.

Directing attention now to the shift of Wohl's experimental curves toward the rich side, the explanation advanced by Wohl and accepted by the present

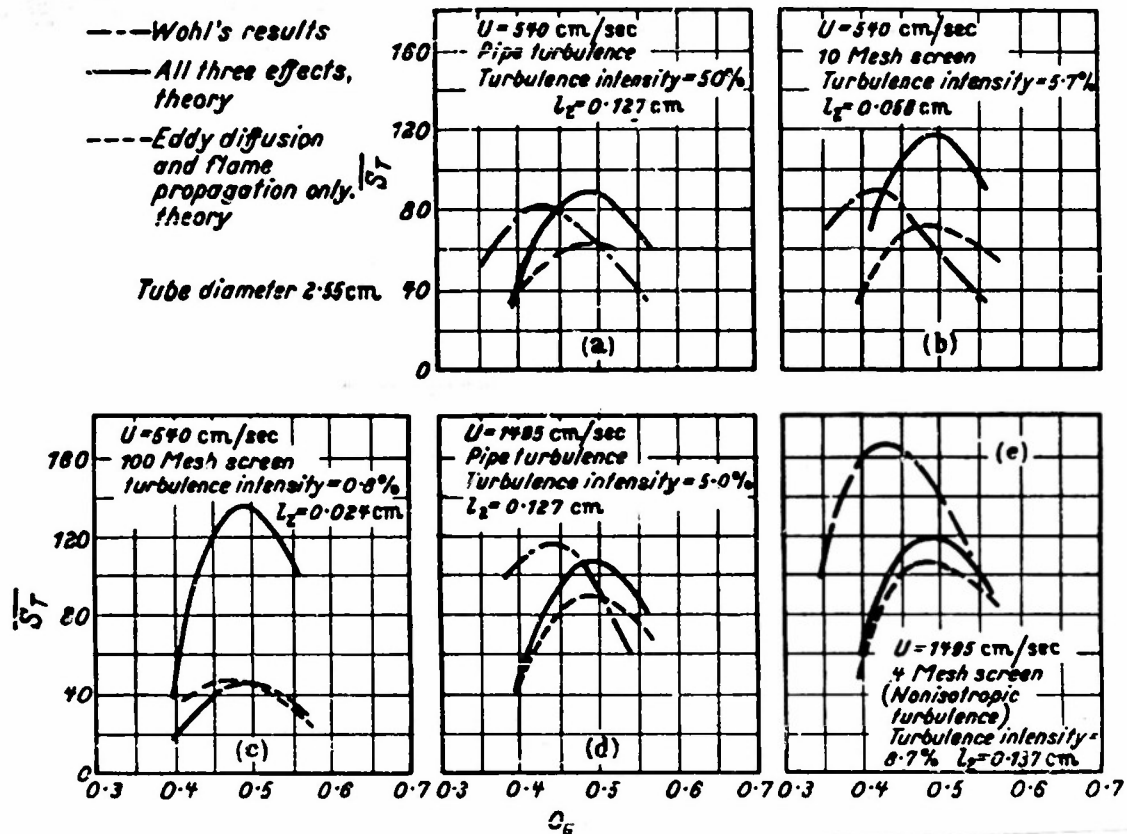


Fig. 23. Experimental results of WOHL and co-workers²³ compared with theory

authors is that polygonal and cellular structures form on the rich-mixture flame surfaces which augment extension of the flame surface by turbulence. Formation of these cells on the surface of laminar flames of rich mixtures of higher hydrocarbons with air is due to the higher diffusivity of the scarce component and is presumably triggered and encouraged by the approach turbulence. This inherent instability of such flames may be thought of as a curvature effect, but one which acts to increase the flame area rather than to flatten and decrease it as before. Another feature of such unstable flame surfaces which has been studied extensively by MARKSTEIN^{17, 20} is their tendency to break down into cells of a size dependent on the composition and state of the mixture. Thus, it might be expected that although the formation of such cells may be triggered by the approach turbulence, the scale of the cells formed would be, at least to a large extent, determined by

the mixture composition and not by the scale of the approach turbulence. Experimental evidence that this is the case has been obtained by WOHL²¹ who found the following results with butane-air bunsen flames disturbed by pipe turbulence ($D = 2.55$ cm) by measuring the average size of the flame distortions (cells) :

O_G	0.521	0.489	0.440	0.419
Average Cell						
Diameter (cm)			0.54	0.50	0.38	0.39

It may tentatively be concluded from these results that the cells which formed on the rich butane-air flame surfaces were smaller than the distortions resulting from eddy diffusion due to approach turbulence, and that the mean cell size was thus reduced. Wohl also has made the observation consistent with the above that the flame brush is, under similar conditions, thinner for the rich butane flames than for those where the mixture ratio is stoichiometric.

The theoretical curves of *Fig. 23* were calculated assuming the size of the flame wrinkles to be proportional to the scale of the approach turbulence. No effect of mixture composition on wrinkle size was included as it would appear unnecessary, at least for rich butane flames. The error toward the low side introduced by failure to make this correction might be expected on the basis of Wohl's above cell-diameter measurements to be greatest with the theoretical results for the four-mesh screen because the assumed scale of the distortions as given by $k_z l_z$ would in this instance be in error on the high side by the largest amount. For the same reasons the calculated results for the 100-mesh screen probably tend to be too high because distortion size based on scale of the approach turbulence would be too low.

Effect of rate of increase of flame area on laminar flame velocity

It has been shown that as a segment of a turbulent flame oriented obliquely to the mean flow moves downstream its area increases. KARLOVITZ, DENNISTON, KNAPSCHAEFER, and WELLS¹³, in considering a laminar flame situated in a flow with velocity gradient, have recently shown that this extension of the flame front tends to decrease the laminar flame velocity S_L to a lower value S_L' . It is desirable to determine quantitatively the importance of this effect on turbulent flames encountered in practice. KARLOVITZ *et al*¹³ derive a relation between S_L'/S_L , the thermal diffusivity of the unburned gases κ , and $(1/U) dU/dy$ which can be readily converted to the following relationship between S_L'/S_L and the rate of change of flame area per unit area, $(1/A) dA/dt$:

$$\int_0^\infty \exp - \frac{S_L'}{S_L} \left[\frac{\eta}{\eta_0} + \frac{\kappa}{2 S_L^2} \cdot \frac{1}{S_L'/S_L} \cdot \frac{1}{A} \cdot \frac{dA}{dt} \left(\frac{\eta}{\eta_0} \right)^2 \right] \frac{d\eta}{\eta_0} = 1 \quad \dots (16)$$

where η is the distance from any point in the unburned gas to the reaction zone of the combustion wave and $\eta_0 = \kappa/S_L$. A plot of S_L'/S_L versus $\left(\frac{\kappa}{S_L^2} \right) \left(\frac{1}{A} \frac{dA}{dt} \right)$ obtained by numerical solution of Eq. (16) is shown in *Fig. 24*.

To determine the importance of this effect in reducing S_L under practical conditions, $(1/A) \frac{dA}{dt}$ versus distance from the stabilizer was calculated for the high-velocity ($v = 301.7$ ft/sec) confined flame of Fig. 10(a) and is shown as the dotted curve in Fig. 11. The maximum value of $\left(\frac{1}{A}\right) \frac{dA}{dt} = 522/\text{sec}$

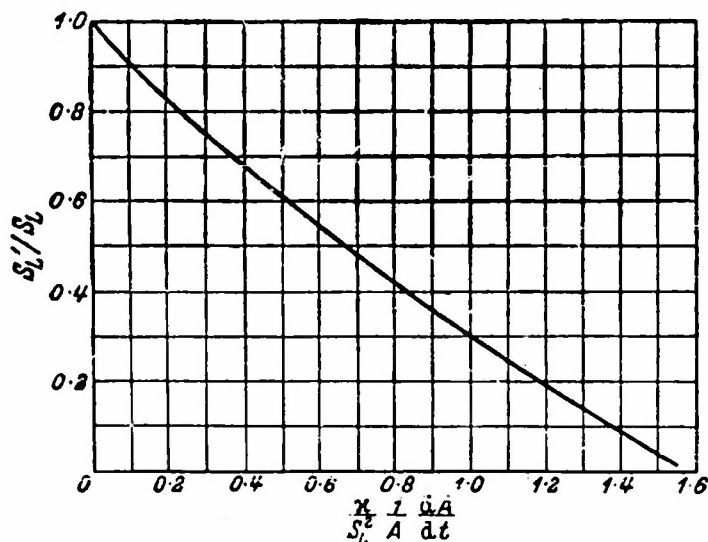


Fig. 24. Relationship between S_L'/S_L and $\frac{x}{S_L^2} \cdot \frac{1}{A} \cdot \frac{dA}{dt}$ from Eq. 16 based on relations developed by KARLOVITZ et al.¹⁸

(based on S_T/S_L determined from the extrapolated flame width curve) occurs at the greatest distance from the stabilizer. Taking S_L as 33 cm/sec and x as 0.2 cm²/sec, the corresponding S_L'/S_L from Fig. 24 is 0.91. Thus, even under these extreme conditions only a nine per cent reduction in S_L due to flame extension is predicted.

Chemical reaction rate may become controlling at very high heat release rates

LONGWELL¹⁵ in a recent paper pointed out that at the high heat release rates sometimes encountered in ram-jet combustion chambers consideration of the necessary flame area per unit volume assuming the high heat release to be associated entirely with an increase in flame area leads to the conclusion that flame front packing would necessarily be so close that interference may be considerable. It was further suggested that under such circumstances the reaction might begin to approach homogeneity and that treatment of turbulent combustion as simple extension of laminar flame front area would no longer be expected to apply. This reasoning has been developed by Avery and Hart² by theoretical consideration of combustion characteristics for instantaneous homogeneous mixing, and it is understood from AVERY¹ that workers at the Esso Laboratories of Standard Oil Development Company and the Applied Physics Laboratory of Johns Hopkins University have operated combustion chambers at enormous volumetric heat release rates in the neighborhood of $500 \times 10^6 \text{ B.T.U./h.ft}^3 \cdot \text{atm}^2$ where performance is approximately that predicted under conditions of instantaneous homogeneous mixing and where chemical reaction rate becomes controlling. This would appear to be a fruitful area for further work.

CONCLUSIONS

The effects of turbulence on turbulent diffusion flames and turbulent flames propagating in homogeneous mixtures appear to be quite different.

Turbulent diffusion flames

For turbulent diffusion flames, it may be concluded that mixing of fuel and oxidant by eddy diffusion is the principal controlling factor determining the rate of burning. The mixing process which controls the combustion of turbulent fuel jets is principally a function of the momentum and buoyancy of the jet, and there is no evidence that the combustion itself results in the generation of additional turbulence. At very high jet velocities, there are indications that molecular diffusion exerts a small limiting effect on the mixing process.

Turbulent flames in homogeneous mixtures

As compared with turbulent diffusion flames the mechanism of propagation of turbulent flames in homogeneous mixtures is more complex and is presently less well understood. For these flames the experimental results useful for comparison with theory are inadequate. Comparison of the limited available results with the theory recently developed by the present authors yields acceptable agreement in some instances and in others the need for further refinement is evident. It is concluded, however, that for the case where the turbulence scale is large compared with flame front thickness the principal necessary elements of a quantitative theory relating the parameters of the approach turbulence and those of the flame to S_T are embodied. On the basis that the increased flame velocity observed in the presence of turbulence results only from an increase in flame area, the theory relates S_T to S_L , l_2 , and \overline{V}^2 by Eq. (4). Three effects are assumed to be of importance in determining the area of the wrinkled flame :

- (1) Eddy diffusion associated with turbulence in the unburned gases, which tends to increase the flame area (by increasing \overline{V}^2) without bound with time, the rate of area increase being made greater by increasing v' , by decreasing S_L , and by decreasing l_2 . The importance of time has been overlooked in the development of previous theories.
- (2) Flame propagation which tends to decrease the flame area (by decreasing \overline{V}^2) and cause it to approach a limiting value which is a direct function of v'/S_L . In practice, however, turbulent flame elements during their short existence usually do not reach this asymptote.
- (3) Flame-generated disturbances which tend to increase the flame area (by increasing \overline{V}^2). From an expression derived for the maximum energy available for development of flame-generated disturbances combined with the assumption that all of this available energy is transformed into isotropic turbulence, it is indicated that the maximum flame-generated turbulence v_m' in practical instances increases approximately as the three-halves power of ρ_u/ρ_b and as the first power of V_u . For confined flames where generally $V_u \gg S_T$, it would be expected,

assuming even a moderate conversion of available energy to turbulence, that v_m' would control in determining S_T . This conforms with experiment. For unconfined flames, on the other hand, the two turbulence intensities are often of the same order.

Desirable refinements of the theory indicated by comparison of theory with experiment include provision for effects of flame curvature and of flame front instability (when it exists) on S_T , and provision for effect of 'flame Reynolds number' on percentage conversion of available energy to turbulence. Additional experiments with turbulent flames are thus required to establish the effects of flame curvature, to gain a more detailed knowledge of the effects of flame front instability, and to determine the contribution of flame-generated turbulence. Extension of existing results to larger scales, results at various ratios of scale to tube diameter and at various values of v'/S_L , and additional study of the instantaneous turbulent flame front should yield needed information. For accurate point determinations of S_T , flow divergence in the unburned gases must be taken into account. Consideration of the mechanism of turbulence generation at regions of shear and experimental observations of flame-generated disturbances suggest that disturbances generated in the wrinkled flame are likely to deviate considerably from isotropy. How this modifies theoretical conclusions based on the assumption of isotropy is unknown and requires experimental determination.

Indications are that flame stretching which generally occurs in flames exposed to turbulence has only a slight effect on S_L , even under extreme conditions.

At enormous volumetric heat release rates of the order of, or above, those sometimes encountered in ram-jet combustion chambers, consideration of the necessary flame area per unit volume assuming the high heat release rates to result only from extension of flame surface indicates that considerable interference may result due to close packing of flame fronts. Treatment of turbulent combustion as simple extension of flame front area may then no longer apply. There are indications, in fact, that under these conditions the reaction approaches homogeneity with chemical reaction rate controlling the combustion process.

FRENCH SUMMARY

Les combustions turbulentes envisagées se rapportent à des flammes de diffusion et à des flammes se propageant dans les mélanges homogènes. En ce qui concerne les premières, on montre d'abord à la lumière des résultats expérimentaux que le processus de la combustion est contrôlé par les phénomènes de mélange, par diffusion tourbillonnaire. En ce qui concerne la propagation des flammes turbulentes en atmosphère combustible homogène finie, on se limite à passer en revue les résultats expérimentaux qui se prêtent à des confrontations théoriques.

On montre l'accroissement de célérité de la flamme à l'apparition de la turbulence, l'accroissement de la distorsion et de la célérité de la flamme quand on s'éloigne vers l'aval du stabilisateur, la structure instantanée caractéristique du front de flamme et, pour des flammes en atmosphère limitée, la création de la turbulence par la flamme.

On compare les résultats expérimentaux à ceux d'une théorie établie précédemment par les auteurs dans le cas d'une turbulence à grande échelle et dont on suppose que le seul effet est de rider le front de flamme sans modifier la célérité S_L de la flamme ; dans cette théorie, qui rattache le rapport $\frac{S_T/S_L}{S_T}$ (célérité apparente de la flamme turbulente) aux paramètres adimensionnels V'/S_L , ρ_u/ρ_b et S_{Lt}/l_t , on tient compte de trois effets : la diffusion tourbillonnaire, la propagation de la flamme et la turbulence créée par la flamme. L'accord entre la théorie et l'expérience est satisfaisant dans certains cas, mais il apparaît que dans d'autres cas il est nécessaire d'ajouter des perfectionnements à la théorie en tenant compte notamment de l'effet sur S_T de la courbure du front de flamme, éventuellement de son instabilité, de l'anisotropie de la turbulence créée par la flamme, enfin l'effet du " Nombre de Reynolds de la flamme " sur la proportion de l'énergie disponible pour créer de la turbulence. Des essais supplémentaires sont nécessaires pour préciser l'importance de ces divers effets : on suggère des expériences qui devraient fournir des résultats intéressants. L'accroissement de surface de la flamme turbulente quand S_L décroît n'agit que modérément dans les cas extrêmes. On discute si dans le cas où la libération de chaleur par la réaction chimique s'effectue à des vitesses très grandes, mais expérimentalement réalisables, le processus de la combustion ne devient pas très proche de celui d'une réaction chimique homogène, la vitesse de la réaction devenant alors le facteur prépondérant.

REFERENCES

- ¹ AVERY, W. H. Private communication, Sept. 1953
- ² — and HART, R. W. *Industr. Engng Chem. (Industr.)* Vol. 45, p. 1634, 1953
- ³ BOLLINGER, L. M. and WILLIAMS, D. T. *Nat. Advisory Comm. Aeronaut. Tech. Note 1707*, 1949 ; *Third Symposium on Combustion, Flame, and Explosion Phenomena*, p. 176 ; Williams & Wilkins, Baltimore, 1949
- ⁴ BURKE, S. P. and SCHUMANN, T. E. W. *Industr. Engng Chem. (Industr.)* Vol. 20, p. 998, 1928
- ⁵ DAMKÖHLER, G. *Z. Elektrochem.* Vol. 46, p. 601, 1940 ; English translation : *Nat. Advisory Comm. Aeronaut. Tech. Memor. 1112*, 1947
- ⁶ DRYDEN, H. L. *Industr. Engng Chem. (Industr.)* Vol. 31, p. 416, 1939 ; *Quart. appl. Mcth.* Vol. 1, p. 7, 1943
- ⁷ GAUNCE, H. Unpublished research on flames, Massachusetts Institute of Technology, 1937
- ⁸ HAWTHORNE, W. R., WEDDELL, D. S. and HOTTEL, H. C. *Third Symposium on Combustion, Flame, and Explosion Phenomena* p. 266 ; Williams & Wilkins, Baltimore, 1949
- ⁹ HOTTEL, H. C. *Fourth Symposium on Combustion* p. 97 ; Williams & Wilkins, Baltimore, 1952
- ¹⁰ — and HAWTHORNE, W. R. *Third Symposium on Combustion, Flame, and Explosion Phenomena* p. 254 ; Williams & Wilkins, Baltimore, 1949
- ¹¹ — WILLIAMS, G. C. and LEVINE, R. S. *Fourth Symposium on Combustion* p. 636 ; Williams & Wilkins, Baltimore, 1953
- ¹² JOST, W. *Z. phys. Chem. A* Vol. 193, p. 332, 1944

- ¹³ KARLOVITZ, BELA, DENNISTON, Jr, D. W., KNAPSCHAEFER, D. H. and WELLS, F. E. *Fourth Symposium on Combustion* p. 613 ; Williams & Wilkins, Baltimore, 1953
- ¹⁴ — — and WELLS, F. E. *J. chem. Phys.* Vol. 19, p. 541, 1951
- ¹⁵ LONGWELL, J. P. *Fourth Symposium on Combustion* p. 90 ; Williams & Wilkins, Baltimore, 1953
- ¹⁶ MALLARD, E. and LE CHATELIER, H. *Ann. Min., Paris* Vol. 8, Ser. 4, p. 274, 1883
- ¹⁷ MARKSTEIN, G. H. *Fourth Symposium on Combustion* p. 44 ; Williams & Wilkins, Baltimore, 1953
- ¹⁸ — *J. chem. Phys.* Vol. 17, p. 428, 1949
- ¹⁹ — *Third Symposium on Combustion, Flame, and Explosion Phenomena* p. 162 ; Williams & Wilkins, Baltimore, 1949
- ²⁰ — and SOMERS, L. M. *Fourth Symposium on Combustion* p. 527 ; Williams & Wilkins, Baltimore, 1953
- ²¹ SCURLOCK, A. C. "Flame Stabilization and Propagation in High-Velocity Gas Streams", Sc.D. Thesis (Chem. Eng.), Massachusetts Institute of Technology, 1948
- ²² — *M.I.T. Fuels Res. Lab., Meteor Rep.* No. 19, July 1948
- ²³ — and GROVER, J. H. *Fourth Symposium on Combustion* p. 645 ; Williams & Wilkins, Baltimore, 1953
- ²⁴ SHELKIN, K. I. *J. tech. Phys., Moscow* Vol. 13, p. 520, 1943 ; English translation : *Nat. Advisory Comm. Aeronaut. Tech. Memor.* 1110, 1947
- ²⁵ TAYLOR, G. I. *Proc. Lond. math. Soc.* Vol. 20, p. 196, 1921
- ²⁶ — *Proc. roy. Soc. A* Vol. 151, p. 421, 1935 ; Vol. 156, p. 307, 1936
- ²⁷ WILLIAMS, G. C., HOTTEL, H. C. and SCURLOCK, A. C. *Third Symposium on Combustion, Flame, and Explosion Phenomena* p. 21 ; Williams & Wilkins, Baltimore, 1949
- ²⁸ — and SHIPMAN, C. W. *Fourth Symposium on Combustion* p. 733 ; Williams & Wilkins, Baltimore, 1953
- ²⁹ WOHL, KURT. *Project Squid Semi-Annual Progress Report* p. 162, Oct. 1, 1952
- ³⁰ — and SHORE, L. Unpublished photographs
- ³¹ — Unpublished work
- ³² — GAZLEY, CARL, and KAPP, NUMER. *Third Symposium on Combustion, Flame, and Explosion Phenomena* p. 288 ; Williams & Wilkins, Baltimore, 1949
- ³³ — SHORE, L., VON ROSENBERG, H. and WEIL, C. W. *Fourth Symposium on Combustion* p. 620 ; Williams & Wilkins, Baltimore, 1953

EXPERIMENTAL STUDIES ON TURBULENT FLAMES

SYMBOLS

A	— area of a flame segment	R_y	— correlation coefficient expressing correlation of the fluctuating velocities at the same time of fluid particles separated by a distance y used in the Eulerian description of turbulence
A_T/A_L	— ratio of wrinkled to initially flat flame area	R_G	— mixed correlation coefficient which expresses correlation between the fluctuating velocity of a flame element at zero time and that of the same element at a later time t after the flame has propagated distance $y = S_L t$
c_1	$= 4K_1^2/K_2^2$	S_L	— laminar flame velocity
c_2	$= 1/2K_1$	S_L'	— laminar flame velocity reduced by rapid increase in flame area
D	— tube or port diameter	S_T	— turbulent flame velocity
E_m	— maximum energy available for conversion to flame-generated turbulence	\bar{S}_T	— average turbulent flame velocity
H	— height of diffusion flame jet	t	— time
K	$= (\frac{\Delta P}{\Delta P'} - 1)$	U	— flow velocity
K_m	$= K$ for $S_T/S_L = \infty$	V_u	— flow velocity normal to the mean flame front
k	— proportionality constant in empirical relation correlating results by Bollinger and Williams	v'	— turbulence intensity defined as root-mean-square fluctuating velocity normal to mean flame front ($= u' = w'$ for isotropic turbulence)
K_1	— proportionality constant relating depth of flame wrinkles to $(\bar{r}^2)^{1/2}$	v'_m	— flame-generated turbulence intensity
K_2	— proportionality constant relating width of scale of flame wrinkles to l_2	v_o'	— approach stream turbulence intensity
L	— distance from stabilizer measured along mean flame front	\bar{r}^2	— mean-square displacement of flame elements normal to the mean flame front
l_1	— Lagrangian scale of turbulence	β	— angle included by flow velocity vector and mean flame front
l_2	— Eulerian scale of turbulence	ϵ	— eddy diffusivity
Q_o	— generalized oxidant fraction $= \frac{\text{oxidant} + \text{oxidant equivalent of fuel}}{\text{oxidant} + \text{oxidant equivalent of fuel}}$	η	— distance into the unburned mixture normal to combustion wave
ΔP	— pressure drop across flame front	η_0	$= \kappa/S_L$
$\Delta P/\Delta P'$	— ratio of pressure drops between the unburned gases and burned unmixed gases, and unburned gases and burned mixed gases	κ	— thermal diffusivity
R	— correlation coefficient expressing correlation of the fluctuating velocities of single fluid particles at zero time and after passage of time t used in the Lagrangian description of turbulence	ν	— kinematic viscosity
		ρ_b	— density of burned gases
		ρ_u	— density of unburned mixture

Armed Services Technical Information Agency

Because of our limited supply, you are requested to return this copy WHEN IT HAS SERVED YOUR PURPOSE so that it may be made available to other requesters. Your cooperation will be appreciated.

AD

38641

NOTICE: WHEN GOVERNMENT OR OTHER DRAWINGS, SPECIFICATIONS OR OTHER DATA ARE USED FOR ANY PURPOSE OTHER THAN IN CONNECTION WITH A DEFINITELY RELATED GOVERNMENT PROCUREMENT OPERATION, THE U. S. GOVERNMENT THEREBY INCURS NO RESPONSIBILITY, NOR ANY OBLIGATION WHATSOEVER; AND THE FACT THAT THE GOVERNMENT MAY HAVE FORMULATED, FURNISHED, OR IN ANY WAY SUPPLIED THE SAID DRAWINGS, SPECIFICATIONS, OR OTHER DATA IS NOT TO BE REGARDED BY IMPLICATION OR OTHERWISE AS IN ANY MANNER LICENSING THE HOLDER OR ANY OTHER PERSON OR CORPORATION, OR CONVEYING ANY RIGHTS OR PERMISSION TO MANUFACTURE, USE OR SELL ANY PATENTED INVENTION THAT MAY IN ANY WAY BE RELATED THERETO.

Reproduced by
DOCUMENT SERVICE CENTER
KNOTT BUILDING, DAYTON, 2, OHIO

UNCLASSIFIED